

Machine learning approaches for lateral strength estimation in squat shear walls: A comparative study and practical implications

Khuong Le Nguyen^{a,b}, Hoa Thi Trinh^a, Saeed Banihashemi^b, Thong M. Pham^{c,*}¹

^a Department of Civil Engineering, University of Transport Technology, Hanoi 100000, Viet Nam

^b Faculty of Arts and Design, University of Canberra, 11 Kirinari St, Bruce, ACT 2617, Australia

^c UniSA STEM University of South Australia, Mawson Lakes, SA 5095, Australia

ARTICLE INFO

Keywords:

Squat shear wall
Machine learning
Ensemble learning
SHAP values
XGBoost
Non-linear pushover analysis

ABSTRACT

This study investigated the influence of input parameters on the shear strength of RC squat walls using machine learning (ML) models and finite element method (FEM) analysis. The analyses were conducted on the largest currently available dataset of 639 squat RC walls with a height-to-length ratio of less than or equal to 2.0. The findings suggest that ensemble learning models, specifically XGBoost, CatBoost, GBRT, and RF, are effective in predicting the shear strength of RC short shear walls and using Bayesian Optimization for hyperparameter tuning improves their performance. The axial load had a greater influence on the shear strength than reinforcement ratio, and longitudinal reinforcement had a more significant impact compared to horizontal and vertical reinforcement. The performance of XGBoost model significantly outperforms traditional design models such as ACI 318-19, ASCE/SEI 43-05, and Wood 1990. Additionally, reducing the number of input features from 13 to 10, 8, or 6 still yields reliable predictions with high accuracy. The finding suggests that the use of XGBoost models provides not only comparable accuracy to FEM simulations with non-linear pushover analysis but also the first one can predict the lateral strength in the case of incomplete data which could not be done by FEM. A web application incorporating XGBoost model with various input features can provide valuable insights for predicting the lateral strength of squat shear walls in building structures.

1. Introduction

Squat shear walls, also known as short reinforced concrete (RC) walls, are commonly used in construction for retaining walls, foundations, and other structural applications (Antoniades et al., 2007; Babaeidarabad et al., 2014; Dan, 2012; Kassem, 2015). The lateral strength of RC walls depends on various factors, such as the type and amount of reinforcement, the dimensions and shape of the wall, the type and properties of concrete, and the axial load (Bekó et al., 2015; Hidalgo et al., 2002; Kotronis et al., 2003). Accurately predicting the strength of these walls enables engineers to design and construct buildings that can withstand the forces while providing adequate protection for occupants (Ning & Li, 2017; Yazgan, 2015). In addition, predicting the lateral strength of reinforced concrete short-shear walls can help to reduce the cost of construction due to over-designing the walls.

Traditional methods such as the modified compressive field theory

(MCFT) (Vecchio & Collins, 1986), cyclic softening membrane model theory (CSMM) (Hsu & Zhu, 2002), and strut-and-tie model theory (STM) (Hwang & Lee, 2002), exhibit limitations in accurately predicting strength. MCFT, for instance, may not effectively capture non-linear concrete behaviour, especially under high-stress levels and complex loading scenarios. This method's accuracy may be compromised when applied to cases with significant nonlinearities, leading to errors of up to 20% in strength prediction (Arabzadeh et al., 2011). CSMM could struggle with strength degradation and stiffness decay prediction under cyclic loading, resulting in errors ranging from 10% to 30% (Feng et al., 2018). On the other hand, STM may be inadequate for complex geometries and strain localisation effects, causing errors of up to 25% in lateral strength predictions (Kassem, 2015).

Additionally, existing semi-empirical formulas for estimating the shear strength of reinforced concrete walls, as specified in ACI 318 (ACI Committee 318, 2022) and EC-8 (EN 1998-1, 2005), are based on the

* Corresponding author.

E-mail addresses: khuongln@utt.edu.vn (K. Le Nguyen), hoatt85@utt.edu.vn (H.T. Trinh), khuong.lenguyen@canberra.edu.au, saeed.banihashemi@canberra.edu.au (S. Banihashemi), thong.pham@unisa.edu.au (T.M. Pham).

¹ <https://orcid.org/0000-0003-4901-7113>.

<https://doi.org/10.1016/j.eswa.2023.122458>

Received 31 May 2023; Received in revised form 2 November 2023; Accepted 3 November 2023

Available online 4 November 2023

0957-4174/© 2023 The Authors. Published by Elsevier Ltd. This is an open access article under the CC BY-NC-ND license (<http://creativecommons.org/licenses/by-nc-nd/4.0/>).

superposition principle and experimental data. The superposition principle is only valid in the linear elastic region while the wall behaviour and also concrete properties are highly non-linear. The adoption of the superposition principle can provide a simple solution but their predictions under non-linear regions are in doubt. Therefore, these design formulas are simple and provide a certain level of safety reserve, but they have not yet provided reliable predictions of the shear strength. These limitations have led to a significant deviation in the estimated shear capacity of short RC walls, highlighting the need for more accurate and reliable methods of prediction.

In recent years, machine learning (ML) approaches have been increasingly applied in civil engineering, particularly in the field of structural analysis (Sun et al., 2021), to predict the behaviour of various structural elements such as beams (Abuodeh et al., 2020; Degtyarev & Tsavdaridis, 2022; Feng, Wang, Mangalathu, Hu, et al., 2021; Le Nguyen et al., 2023), slabs (Elshafey et al., 2011; Le Nguyen et al., 2023; Tran & Kim, 2021), and columns (Cascardi et al., 2017; Hou & Zhou, 2022; Junda et al., 2023; Le-Nguyen et al., 2022; Naderpour et al., 2010). Among these trends, ML approaches have been successfully used to predict the lateral strength of RC walls. Feng et al. (2021) developed a predictive model using the extreme gradient boosting algorithm to estimate the shear strength of squat walls and obtained a reasonable prediction accuracy. Chen et al. (2018) and Nguyen et al. (2021) also employed artificial neural networks (ANNs) to predict the shear strength of squat walls, yielding satisfactory results. Gondia et al. (2020) used genetic programming to predict the shear strength of flanged squat walls and obtained good accuracy and applicability. Keshtegar et al. (2022) developed a hybrid ML model using ANNs coupled with an adaptive harmony search optimisation algorithm to predict the lateral strength of RC walls with superior performance. Studies have also used ML to solve partial differential equations in computational mechanics, which can provide potential alternatives for estimating the performance of RC walls under various loads (Keshtegar et al., 2021; Sadeh & Tehrani-zadeh, 2021). Zhang et al. (2022) devised ML-based models for seismic performance prediction in RC walls, outperforming existing design formulas in accuracy and efficiency. A user-friendly platform was developed for practical RC wall design. While machine learning methods have shown success in numerous studies, challenges still hinder their widespread application in predicting the lateral strength of squat shear walls in the industry. This study identifies and addresses these challenges as follows:

- (i) The first challenge is selecting appropriate and effective models for predicting the lateral strength of reinforced concrete (RC) walls. Previous studies have made different recommendations and suggestions, some indicating that XGBoost performs best (Feng et al., 2021), while others found that alternative methods, such as artificial neural networks (ANNs), yield more accurate results (Chen et al., 2018; Nguyen et al., 2021). This inconsistent statement may be due to a lack of comprehensive comparison of different algorithms. To address this inconsistency, this study conducts a comprehensive comparison of various ML models' performance to provide guidance for practitioners in the field.
- (ii) The second challenge lies in determining the optimal set of input features for predicting the shear strength of RC walls using machine learning. Although several input parameters could be considered, there is limited research examining the effect of different input features on ML algorithms' performance. This study addresses this gap by performing a thorough analysis of input features' influence on the performance of different ML algorithms, which is crucial for practical applications.
- (iii) While prior research primarily compared ML performance against practical codes, fewer studies have integrated the Finite Element Method (FEM) for such evaluations. Recognising this research opportunity, our study adopts a non-linear material model for concrete shear behaviour. This advancement facilitates

automated FEM simulations, laying the groundwork for a comprehensive juxtaposition of FEM and ML model outputs, aiming to combine the rigour of traditional methods with the efficiency of modern data-driven approaches

- (iv) Lastly, although employing ML techniques for predicting the lateral strength of RC walls has the potential to enhance industry productivity, there are limited options for user-friendly platforms that allow designers to conveniently utilise the results from these techniques in real design process. This study develops a web-based app incorporated the trained ML model for predicting the shear strength of squat RC shear walls. This app is available to all users to further disseminate this work to a wider civil engineering society.

2. Methodology

The objectives of this research are outlined in Fig. 1. In this study, we have compiled an extensively curated dataset that encompasses 639 squat RC walls with a height-to-length ratio of less than or equal to 2.0. Owing to its diverse sources, thorough validation processes, and a keen focus on comprehensiveness, this dataset is positioned as one of the more substantive collections available in this domain. Ten different machine-learning models, including Linear Regression (LR), Support Vector Machine (SVM), K-Nearest Neighbors (KNN), Artificial Neural Network (ANN), Decision Tree (DT), Random Forest (RF), Gradient Boosted Regression Trees (GBRT), AdaBoost, CatBoost, and XGBoost.

To conduct the advanced analysis process, the four best-performing models were optimised using Bayesian Optimization which leverages a probabilistic model to determine the ideal set of hyperparameters. Then, the importance level of input parameters was analysed using the SHAP Value method based on XGBoost model, which assigns a score to each input parameter reflecting its contribution to the model's prediction. Additionally, three subdatabases with varying numbers of input features were proposed and investigated. Monte Carlo simulations were employed to evaluate the impact of the number of input features on the performance of the models, providing further insight into the significance of each parameter in the prediction process.

The results of the machine-learning (ML) models were compared to semi-empirical models based on current standards and FEM simulation to demonstrate the predictability and reliability of the machine-learning approach, and the best models were ultimately implemented online for practical application.

This section presents a brief introduction of the adopted ML algorithms, along with the performance indices of the models. The determination of the shear strength of squat shear walls using practical code and FEM simulation is also described.

2.1. Brief introduction of ML algorithms

In this study, a variety of popular and robust machine learning techniques were employed, including Linear Regression (LR), Support Vector Machine (SVM), K-Nearest Neighbors (KNN), Artificial Neural Network (ANN), Decision Tree (DT), Random Forest (RF), Gradient Boosted Regression Trees (GBRT), AdaBoost, CatBoost, and XGBoost. These models have demonstrated strong performance in numerous applications across various fields (Thai, 2022).

Linear regression (LR) (Pedregosa et al., 2011) Support Vector Machine (SVM) (Cortes & Vapnik, 1995) K-Nearest Neighbors (KNN) (Deng et al., 2009) are fundamental machine learning techniques used for regression and classification tasks. Artificial Neural Network (ANN) (Hochreiter & Schmidhuber, 1997) is inspired by biological neural networks and has a wide range of applications, including classification, regression, and feature learning. Decision Tree (Quinlan, 1986), (Pedregosa et al., 2011), and Random Forest (Breiman, 2001) are tree-based methods used for classification and regression problems. Both techniques construct decision trees to predict target variables based on

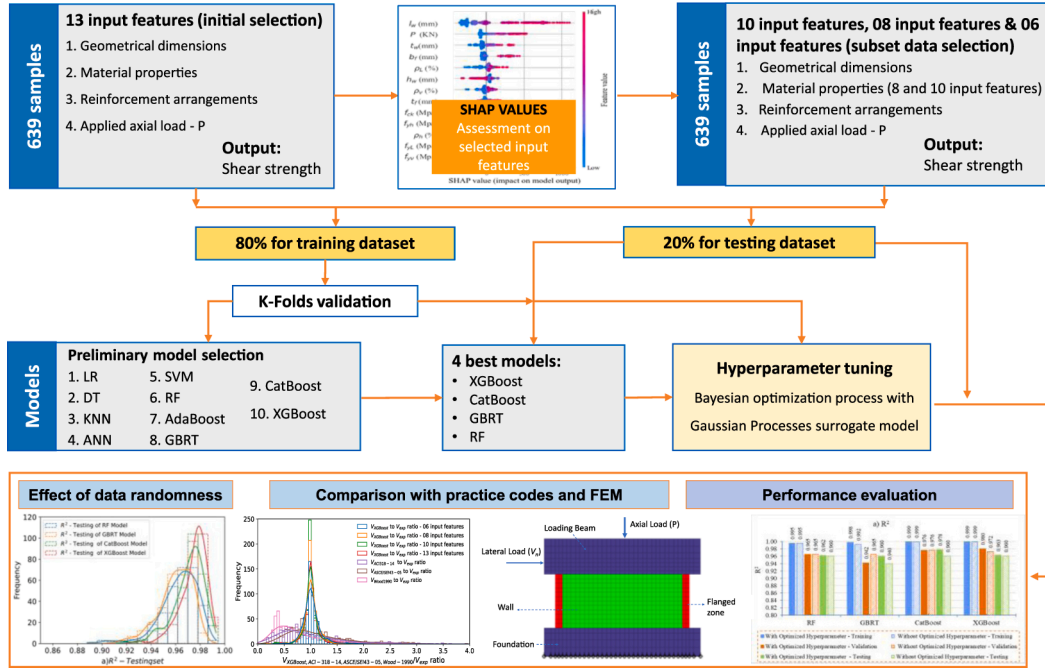


Fig. 1. Outlines of the current research.

data features.

Gradient Boosted Regression Trees (GBRT) (Hastie et al., 2001), AdaBoost (Collins et al., 2000), CatBoost (Dorogush et al., 2018), and XGBoost (Chen & Guestrin, 2016) are ensemble methods that combine multiple weak models to create a strong model. These techniques iteratively improve the model by focusing on areas where previous models underperformed. Among these, CatBoost and XGBoost are particularly efficient gradient boosting libraries designed for large datasets and have gained popularity in structural engineering (Thai, 2022).

2.2. Performance indices of models

To assess the performance of the ML-based models, four statistical indices, including the coefficient of determination (R^2), root mean square error (RMSE), mean absolute error (MAE), and mean square error (MSE), were employed. Accordingly, the smaller the MSE, RMSE, and MAE values, the better the prediction model. Meanwhile, R^2 varying from 0 to 1 indicates the correlation between the actual and predicted values, which means the higher R -value implies a strong correlation between the inputs and output. The formulations of four indices are presented below.

$$\text{Mean Absolute Error } MAE = \frac{1}{N} \sum_{j=1}^N |p_j - p_{t,j}| \quad (1)$$

$$\text{Root Mean Square Error } RMSE = \sqrt{\frac{1}{N} \sum_{j=1}^N (p_j - p_{t,j})^2} \quad (2)$$

$$\text{Coefficient of Determination } (R^2) = 1 - \frac{\sum_{j=1}^N (p_j - p_{t,j})^2}{\sum_{j=1}^N (p_j - \bar{p})^2} \quad (3)$$

$$\text{Mean Square Error } MSE = \frac{1}{N} \sum_{j=1}^N (p_j - p_{t,j})^2 \quad (4)$$

where p_j is the shear strength of j -th actual value in the dataset; $p_{t,j}$ is the shear strength of j -th predicted value obtained from the ML model; \bar{p} is the mean actual value of the shear strength compliance; \bar{p}_t is the mean

predicted value of the shear strength; And N is the total number of samples in the dataset.

2.3. Determining lateral strength of shear walls using semi-empirical codes

Three mechanics-based semi-empirical shear strength models, two from current design codes, including ACI 318-19 (2022), ASCE/SEI 43-05 (2005) and one popular model from the literature (Wood, 1990), were also adopted for comparisons to examine the prediction accuracy of XGBoost relative to the state-of-the-art.

• ACI 318 – 19

$$V_n = (\alpha_c \lambda \sqrt{f_{ck}} + \rho_h f_{yh}) A_{cv} \leq 0.83 \sqrt{f_{ck}} A_{cw} \quad (5)$$

where α_c is the aspect ratio coefficient, which varies linearly in the range 0.25 ($h_w/l_w \leq 1.5$) to 0.17 ($h_w/l_w \geq 2.0$) and varies linearly between 0.25 and 0.17 for h_w/l_w between 1.5 and 2.0 (wall length – l_w , wall height – h_w); λ is a modification factor reflecting concrete properties and equals 1.0 for normal-strength concrete; A_{cv} is the gross area of a concrete section bounded by the web thickness and length of the section in the direction of the considered shear force; and A_{cw} is the gross section area of the wall;

• ASCE/SEI 43 – 05

$$V_n = v_n d t_w \quad (6)$$

$$v_n = 0.69 \sqrt{f_{ck}} - 0.28 \sqrt{f_{ck}} \left(\frac{h_w}{l_w} - 0.5 \right) + \frac{P}{4 l_w t_w} + \rho_{se} f_{yh} \leq 1.66 \sqrt{f_{ck}} \quad (7)$$

$$\rho_{se} = A \rho_v + B \rho_h \quad (8)$$

where $d = 0.6 l_w$; ρ_{se} is the equivalent reinforcing ratio combining ρ_h and ρ_v with coefficients $A = 1$; $B = 0$ for $h_w/l_w \leq 0.5$; $A = -h_w/l_w + 1.5$; $B = h_w/l_w - 0.5$ for $0.5 \leq h_w/l_w \leq 1.5$; and $A = 0$; $B = 1$ for $h_w/l_w \geq 1.5$.

• Wood 1990

$$0.5 \sqrt{f_{ck} A_{cv}} \leq V_n = \frac{A_{vf} f_{yv}}{4} \leq 0.83 \sqrt{f_{ck} A_{cv}} \quad (9)$$

where A_{vf} is the total area of the shear-friction reinforcement - representing the steel reinforcement provided along the wall's height to improve its shear strength ($A_{vf} = \rho_v * A_{cw}$). f_{ck} is the concrete compressive strength, f_{yv} is web vertical steel reinforcement yield strength, A_{cw} is the gross section area of the wall. A_{cv} is the gross area of a concrete section bounded by the web thickness and length of the section in the direction of the considered shear force.

It can be observed that the ACI 318 model does not consider the axial load (P) in its formulation, potentially limiting its applicability in certain structural scenarios. In contrast, Wood's model incorporates the axial load effect, but its upper bound is substantially smaller than that of ASCE/SEI 43-05, which might lead to highly conservative predictions. ASCE/SEI's model provides a comprehensive framework for predicting the lateral shear strength, accounting for various factors such as the axial load and reinforcement ratios. By comparing the performance of these three models against XGBoost model, this study aims to highlight the advantages of employing machine learning techniques for predicting the lateral strength of squat shear walls.

2.4. Finite element method for RC walls simulation

A two-dimensional numerical model was built using open-source code Cast3M (Le Fichoux, 2011). The mesh was simplified to the mid-plane of the wall, with material properties representing a single unit of thickness. Concrete was modelled with four-node membrane elements featuring bilinear displacement interpolation (four Gauss points), while steel reinforcement was represented by two-node bar elements. The influence of mesh size on the results depends on the material model used for non-linear behaviour, specifically the Beton-INSa model. Consequently, following the process proposed in a thesis by Le Nguyen (2015), the mesh size of concrete and steel elements was recalculated automatically for each wall in the database. This approach aimed to maintain accuracy in the representation of each wall's material properties and behaviour, taking into account the specific characteristics and dimensions of individual walls. By adapting the mesh size according to the unique attributes of each wall, the numerical model's predictive capability was enhanced while minimising potential errors associated with fixed mesh sizes. The model description is illustrated in Fig. 2.

The foundation and loading beam were modelled as elastic materials, while the wall was modelled using the non-linear Beton-INSa model, which was based on the theory of plasticity. The complex behaviour of the wall was characterised by two failure surfaces based on Nadai criteria for compression and tension and includes non-linear behaviour in the compression range before cracking, which was governed by a plasticity model based on Nadai threshold function. The concept of fixed

and distributed cracking was used to describe the behaviour of cracked concrete, and when the failure surface in the tension range was reached, the biaxial plasticity was discontinued and an orthotropic law was activated. Djerroud (1992) and Merabet (1990) developed the theoretical foundations and initial implementations of the material behaviour model for concrete material, referred as Beton-INSa. This model has been validated against various structures, including shear walls (Ile & Reynouard, 2000), (Brun et al., 2003, 2004), and shear walls strengthened by FRP by Le Nguyen et al., (2014, 2017), and shows reliable prediction.

More specifically, the INSA concrete model has five main parameters, including Young's modulus, tensile strength, and compressive strength, the plastic deformation at failure in compression, and especially the plastic deformation at failure in tension, which plays a crucial role in controlling crack development. After the compression or tension peak, the behaviour becomes softening, which makes the results sensitive to mesh refinement. A standard regularisation technique called Hillerborg approach (Hillerborg et al., 1976) is adopted, based on the tensile cracking energy or compressive failure energy. The parameters of plastic deformation at failure in tension and compression become dependent on these energies, which are considered intrinsic to the material, as well as a characteristic length obtained from the mesh and the type of finite element. The procedures for calculating failure deformations were detailed in the previous research conducted by Brun et al. (2011) and Le Nguyen et al., (2014, 2017), which are not repeated here for brevity.

The step by step (PASAPAS in French) procedure was used for static pushover analysis by imposing displacement on the loading beam. The load (horizontal reaction) – displacement (horizontal displacement of the top point of the wall) curve will be determined as the result of the non-linear pushover simulation. The lateral strength of each wall will be determined as the maximum value on the pushover curve. The loading rate in the numerical analysis was the same as those in the experiments. As this was a non-linear simulation, the analysis of each wall was stopped when a non-converged problem occurs.

3. Data description

A typical schematic diagram of the squat RC wall tests in the database is shown in Fig. 3. There are four input categories, namely, geometric dimensions, reinforcement arrangements, material properties, and applied axial load. The detailed input features are the height h_w , length l_w , web thickness t_w , flange length b_f , flange thickness t_f , concrete compressive strength f_{ck} , vertical web reinforcement ratio ρ_v and web vertical steel reinforcement yield strength f_{yv} , horizontal web reinforcement ratio ρ_h and web horizontal steel reinforcement yield strength f_{yh} , longitudinal reinforcement ratio ρ_L and boundary element steel reinforcement yield strength f_{yL} , and the applied axial load P . The output

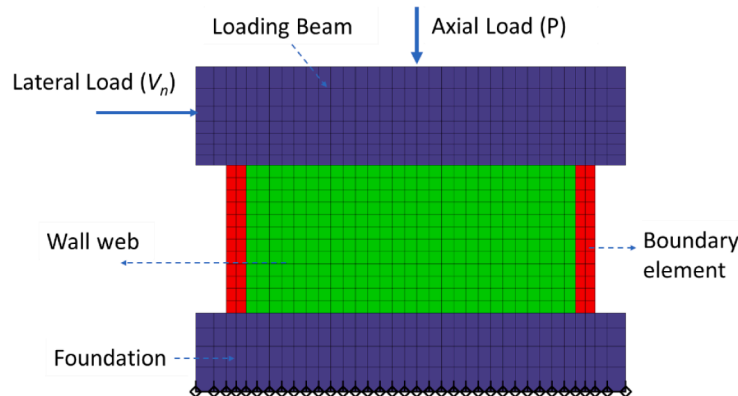


Fig. 2. FEM model of a typical squat RC shear wall.

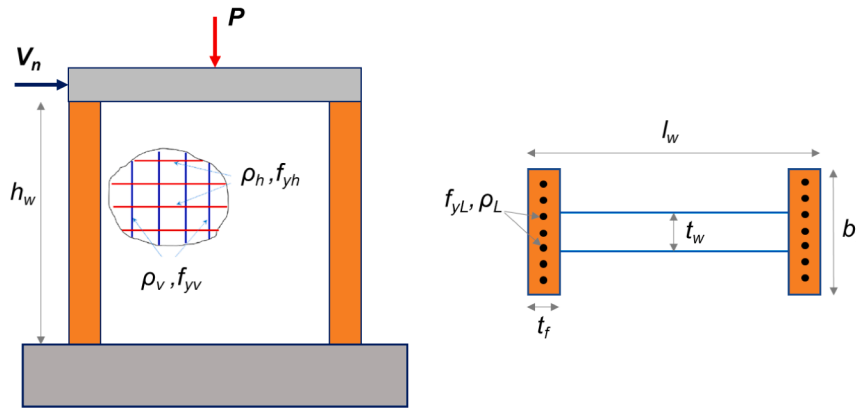


Fig. 3. Schematic diagram of squat RC wall tests.

is the shear strength V_{exp} .

A total of 639 squat RC Walls test data samples were collected, of which 252 specimens were from Massone & Melo (2018), 182 specimens from Ning & Li (2017), 22 specimens were from Sato et al. (1989), 1 specimen was from Baek et al. (2017), 4 specimens were from (Teng & Chandra, 2016), 1 specimen was from Sittipunt & Wood (1993), 25 specimens were from Vallenat et al. (1979), 129 specimens were from Hirose (1975), 7 specimens were from Barda et al. (2011), and 16 specimens were from Whyte & Stojadinovic (2013).

Fig. 4 shows a histogram of the input features that were created as an adjunct to the statistical analysis. The trends and patterns in the data can be seen from this histogram, which graphically displays the frequency distribution of the input features. In summary, the majority of the height of the wall falls in the range of 500 and 1200 mm, with a high frequency centred around 800 mm. The length of the wall varies around 1200 mm, while the width of the web is around 100 mm, and the compressive strength of concrete varies around 30 MPa. The horizontal and vertical reinforcement ratio is around 1%, while the reinforcement ratio in the flanged area is around 3%. The steel tensile strength is approximately 350 MPa. Additionally, some walls are without either vertical reinforcement ($\rho_v = 0$) or horizontal reinforcement ($\rho_h = 0$).

Fig. 5 presents the correlation matrix of features of the original data set, which includes 13 input variables and one output variable. The matrix displays the correlation coefficients between each pair of variables, with a value of 1 indicating the highest positive correlation, a value of -1 indicating the lowest negative correlation, and a value of 0 indicating no correlation. The correlation matrix illustrates the relationship between different variables and how they are related to each other. The initial analysis suggests that there are positive and negative correlations between variables. Pairs of attributes with a high degree of correlation are more dependent on each other. Specifically, the correlation coefficients between reinforcement ratios ρ_v and ρ_h , as well as between f_{yv} and f_{yh} , are the highest at 0.92 and 0.82, respectively.

4. Machine learning implementation and results

The LR, ANN, and SVM models were implemented using Statistics and Machine Learning Toolbox in Matlab, while the DT, KNN, RF, AdaBoost, GBRT, CatBoost, and XGBoost models were implemented using the Scikit-Learn library (Pedregosa et al., 2011).

The entire dataset was divided into a training set of 80% of the data and a test set of 20% of the data. The training set was used to train and fine-tune the predictive models, while the test set was used to evaluate the performance of the models. The models were initially implemented using their default hyperparameters to evaluate model selection. For example, the SVM model used a linear kernel with a cost parameter of $C = 1$ and gamma $= 1/n$ features.

The K-folds cross-validation method was utilised to minimise the

variation of the results and provide a more precise assessment of the model's overall performance. In this study, the training data set was split into ten subsets or "folds" using this approach. Each fold was trained and tested separately, and the mean of ten assessments was used to determine the model's overall performance.

4.1. Performance evaluation of models with default hyperparameters

Performance of the predictive models with default hyperparameters on the training, validation and test datasets is summarised in Fig. 6 and Annex 1. Most of the ML-based models performed well on all the three datasets. The performance of ensemble learning models such as RF, GBRT, CatBoost, and XGBoost was superior to that of standard single-method learning models such as LR, DT, ANN, KNN, and SVM. The CatBoost and XGBoost models exhibited the best training performance based on the coefficient of determination, with the CatBoost model having an R^2 value of 0.999 for the training set, 0.976 for the validation set, and 0.960 for the test set. The RMSE values for the CatBoost model were 18.69, 105.84, and 115.09 for the training, validation, and test sets, respectively. XGBoost model had an R^2 value of 0.999 for the training set, 0.972 for the validation set, and 0.960 for the test set. The RMSE values of XGBoost model were 3.46, 111.80, and 115.49 for the training, validation, and test sets, respectively. Except for the Adaboost model, ensemble learning models such as RF, GBRT, CatBoost, and XGBoost performed well on both the validation and testing datasets. In the subsequent steps, these four models were chosen for additional hyperparameter optimisation and investigation.

4.2. Tuning hyperparameters

Tuning the hyperparameters of a ML model is an essential step in the model-building process, as it can significantly impact the model's performance by reducing overfitting, increasing generalisation, and improving the model's ability to adopt new data. In most cases, the default values for the hyperparameters are not optimal for a specific dataset; thus, tuning is necessary to achieve the best performance.

In this study, Bayesian Optimisation technique was used to fine-tune the hyperparameters of four best-performing ML models, i.e. RF, GBRT, CatBoost, and XGBoost. Bayesian Optimisation is a robust optimisation algorithm that is particularly useful for black-box functions, such as ML models, where the function to be optimised is unknown and cannot be analytically maximised (Snoek et al., 2012). More specifically, Bayesian Optimization algorithm uses a probabilistic model to represent the function to be optimised and updates the model with the results of the evaluations of the function. The algorithm then uses the updated model to guide the search for the global maximum of the function.

The open-source library, scikit-optimize (<https://scikit-optimize.github.io/stable/>, 2020) was used to conduct Bayesian Optimization

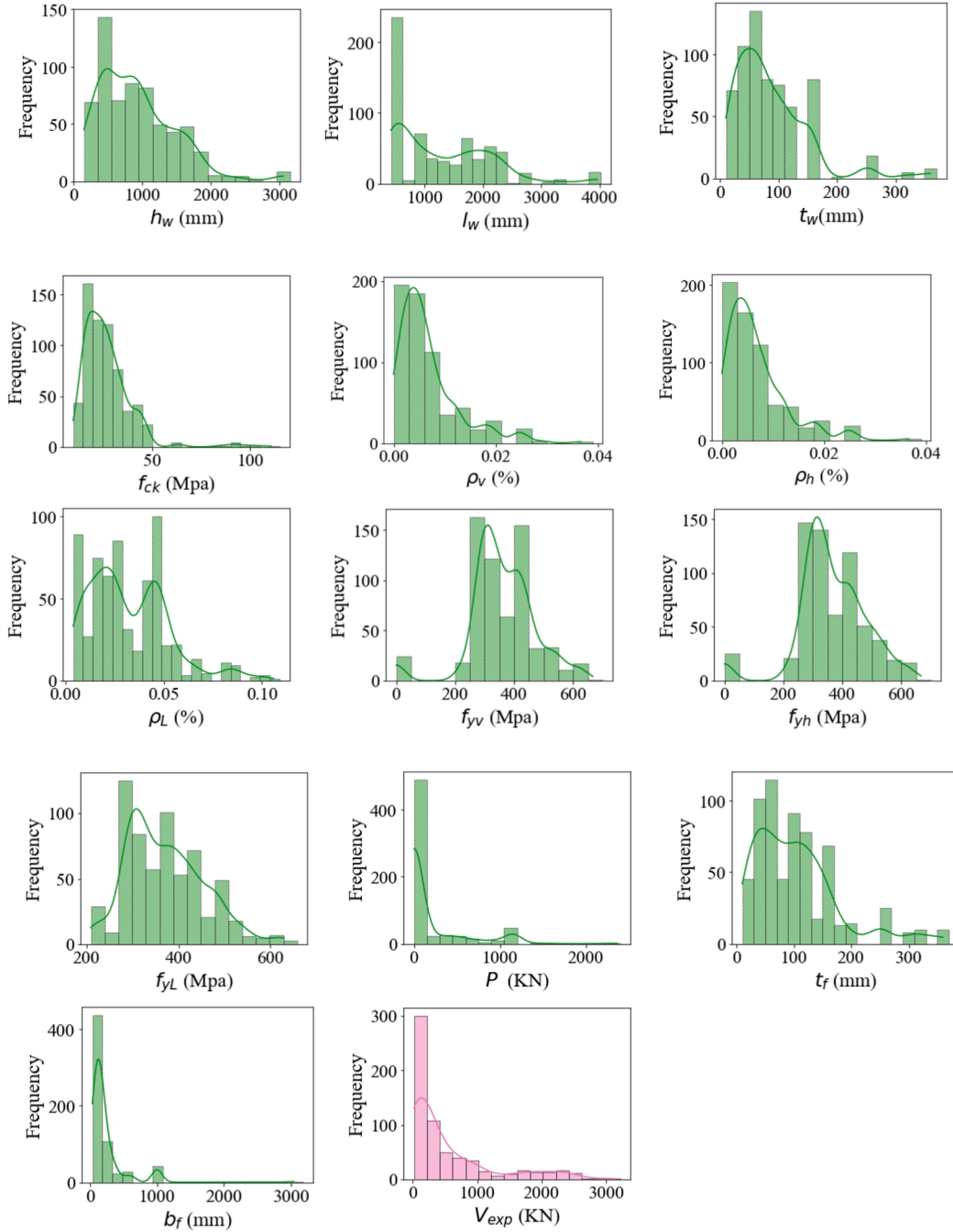


Fig. 4. Histogram of the input features and output.

process, concerning the hyperparameters of the four models to minimise the MSE value on the validation dataset. The optimisation was performed for a maximum of 100 iterations, with each iteration comprising a maximum of 20 function evaluations. The hyperparameters that resulted in the smallest MSE value on the validation dataset were then used to evaluate the performance of the models on the test dataset.

Fig. 7 illustrates the convergence curves of the hyperparameter tuning process for XGBoost, CatBoost, GBRT, and RF models with the ranges and optimised values for the four developed ML models are synthesised in Annex 2. It is worth noting that XGBoost and CatBoost models achieved an MSE value of 12,110 (kN^2) after only 11 iterations, after which the CatBoost model did not change the MSE for the subsequent iterations, while XGBoost model still changed the MSE reduction down to 9,660 (kN^2) at the 30th iteration, which was also the minimum

MSE value of XGBoost. On the other hand, the GBRT and RF models reached the minimum MSE value at the 65th iteration with corresponding values of 17,146 (kN^2) and 16,275 (kN^2), respectively. Overall, the three models, i.e., XGBoost, CatBoost, and RF, all achieved MSE values close to the minimum value after only 11 iterations. GBRT model showed the most variation in MSE values across iterations, and XGBoost model achieved the smallest MSE index among the four models.

4.3. Performance evaluation of hyperparameter optimisation

The effectiveness of using optimised hyperparameters was evaluated by comparing the ML results when using hyperparameters with and without optimisation. The combined results for the four models are shown in Fig. 8.

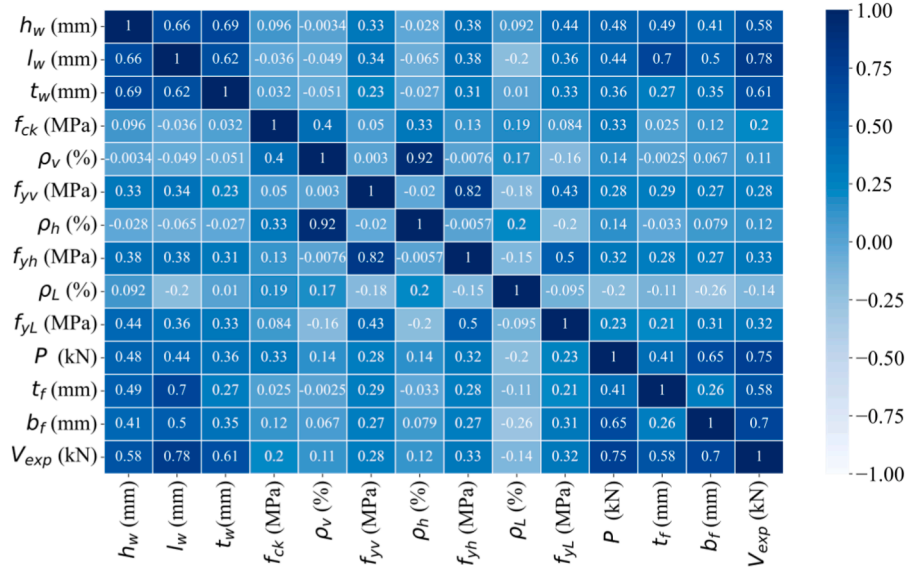


Fig. 5. Correlation matrix of the Features.

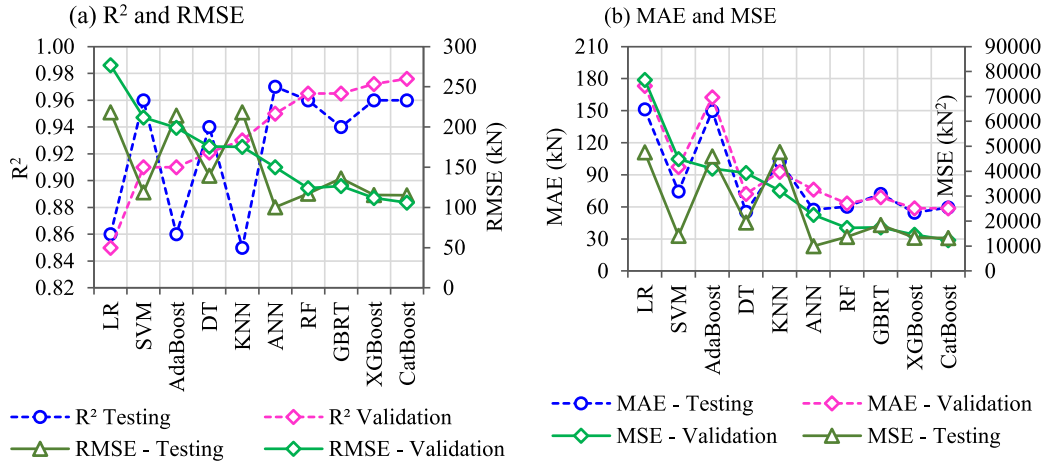


Fig. 6. Performance metrics comparison for ten ML models with default hyperparameters.

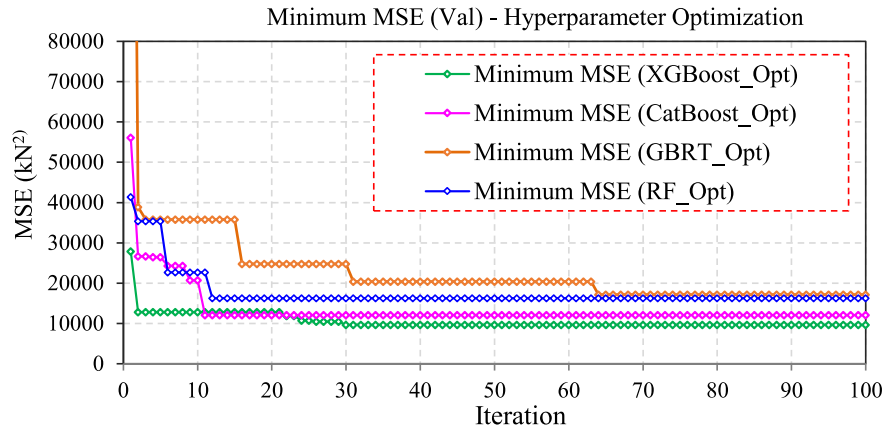


Fig. 7. Minimum MSE converged curve of the optimisation of the hyperparameters process.

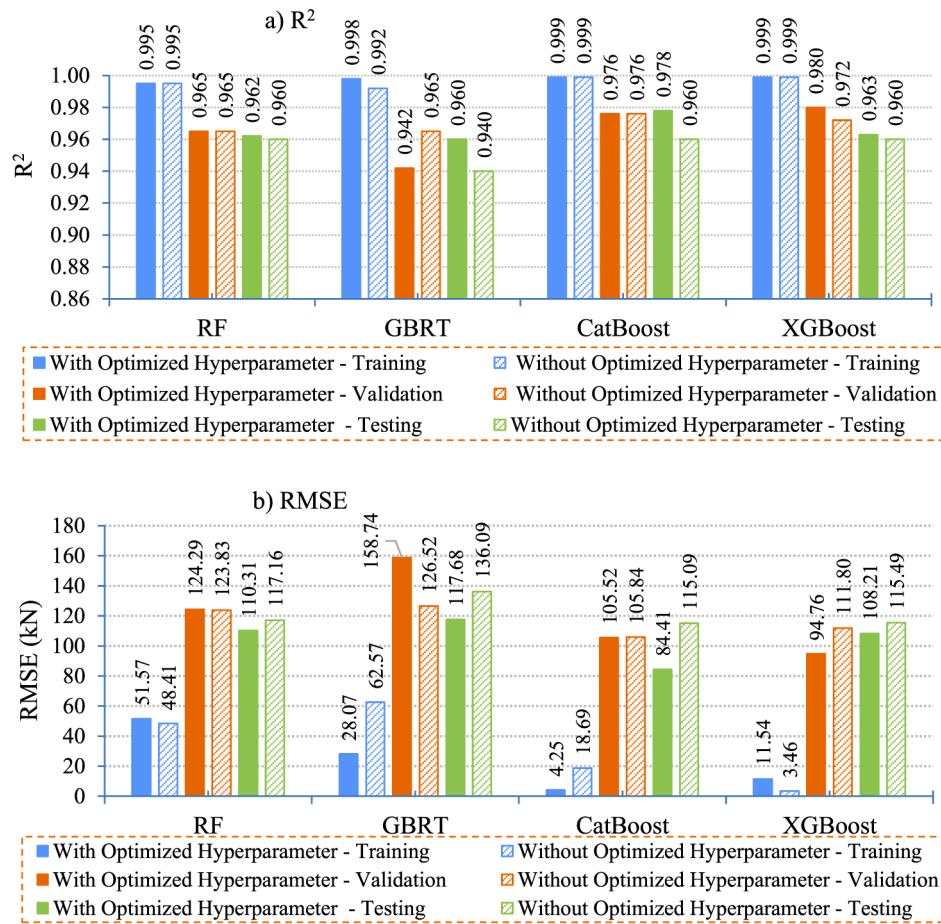


Fig. 8. Comparison of optimisation of the models with and without optimised hyperparameters.

The results indicate that optimisation on the four models, i.e. XGBoost, CatBoost, GBRT, and RF, improves their performance. Specifically, during the training phase, R^2 value showed an improvement, from 0.992 to 0.998 for GBRT model. For the CatBoost, XGBoost, and RF models, the R^2 value did not change. During the validation process, R^2 value remained unchanged for RF and CatBoost models while it increased from 0.972 to 0.980 for XGBoost model. GBRT model showed a decrease in R^2 index, from 0.965 to 0.942 when compared to the non-optimised model. In the testing phase, R^2 of all the four models increased from 0.940 to 0.960 for GBRT model, from 0.960 to 0.962 for RF model, from 0.960 to 0.978 for CatBoost model, and from 0.960 to 0.963 for XGBoost model. In general, even though these models have already shown high performance prior to optimisation, all the optimal models exhibited better performance than the initial models.

Fig. 9 compares the predictions of the four optimised ML models for the shear strength of squat walls against the experimental data. Overall, the four models reliably estimated the shear strength of squat walls. These models achieved high prediction accuracy, with R^2 values higher than 0.96 for both the training and testing datasets. The optimised CatBoost model had the highest prediction accuracy among the four models, with R^2 , RMSE, and MAE values of 0.999/0.978, 4.25/84.41, and 2.68/49.30 for the training and testing datasets, respectively.

4.4. Influence of data randomness via Monte Carlo simulation

In this section, the influence of data randomness on the performance of ML models was evaluated using Monte Carlo simulation (Castaldo et al., 2017) to analyse the robustness and reliability of models by running multiple simulations and obtaining multiple training–testing

splits. The four most reliable models, RF, GBRT, CatBoost, and XGBoost, were employed to train these data subsets, which included 13 input features. At each simulation, the entire database was divided randomly into a training set and a testing set with a proportion of 80% and 20%, respectively. The model was then trained using the training data set and subsequently tested on the testing data set. This process was repeated 300 times with different randomly selected subsets of data, resulting in 300 different training–testing splits. In total, there were $4 \times 300 = 1,200$ simulations. The results of these simulations, including the frequency and convergence of R^2 and RMSE, are presented in Fig. 10.

The aggregate results in Table 1 demonstrate that XGBoost, CatBoost, GBRT, and RF models exhibit convergent and stable predictions over 300 simulations with different data subsets. XGBoost model stands out as the most stable, with a range of R^2 values for the test set varying from 0.927 to 0.993. CatBoost model follows closely, with a range of R^2 values for the test set varying from 0.918 to 0.991. GBRT model also exhibits stability with a range of R^2 values for the test set varying from 0.909 to 0.986, and RF model with a range of R^2 values for the test set varying from 0.888 to 0.991. These results indicate that XGBoost, CatBoost, GBRT, and RF models are robust to the randomness of the data subsets and can achieve stable and consistent performance across different training and testing splits.

To determine the stability of the model, the difference between the R^2 indices of the train set and test set was examined. Table 2 and Fig. 11 reveal that the deviation (Δ) between R^2 value of the training and test sets was consistently positive, relatively small, and remains stable across 300 random data splits for all the four models. The most significant R^2 deviation between training and testing was 0.108 for RF model, indicating a slightly inferior performance on the test dataset compared to the

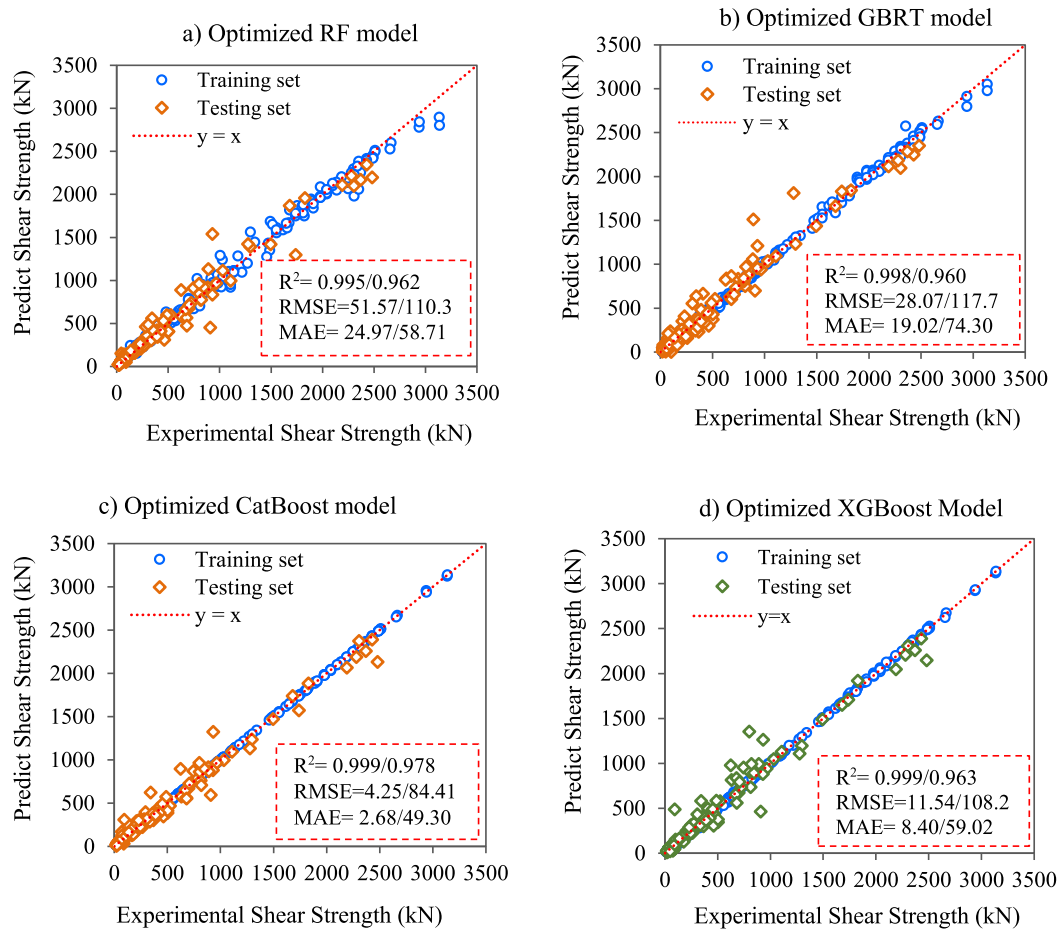


Fig. 9. Predicted shear strength by four optimised models. Note: the value, for example, $R^2 = 0.999/0.978$, represents the model's performance on the training and testing datasets, respectively.

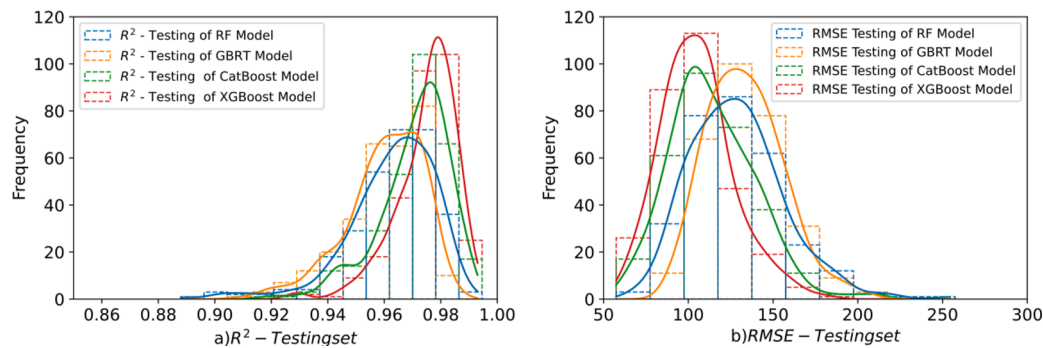


Fig. 10. Histogram of R^2 and RMSE for four models after 300 simulations.

training dataset. On the other hand, XGBoost model gives the smallest and most stable mean deviation of the four training models, with mean of $\Delta = 0.025$, which means that the model's performance on the test dataset was very close to its performance on the training dataset. These results align with the notion that a good model should have a low deviation between training and test R^2 values, indicating good generalisation abilities (Bengio & Grandvalet, 2004).

5. Optimisation of input features for ML models

SHAP technique (Lundberg & Lee, 2017) is based on the Shapley

values from cooperative game theory, and it calculates the average marginal effect of each feature based on all possible feature combinations. The absolute value of SHAP can be used to determine the relative importance of each input feature, where the input features with higher SHAP values indicate a more significant impact on the output.

This section examines the optimisation of input features, which is based on XGBoost model. Moreover, Monte Carlo simulations are used to analyse three subdatabases with varied quantities of input features. This process examines the influence of the number of inputs on the performance of the models and the determination of the optimal number of input features for predicting the lateral strength of squat shear walls.

Table 1

Statistic results for 300 randomisations for four models.

Models	Case	R ² - Training	R ² - Testing	RMSE - Training	RMSE - Testing
RF	Min	0.992	0.888	43.91	68.46
	Max	0.996	0.991	60.32	254.33
	Mean	0.994	0.963	51.80	128.53
GBRT	Min	0.997	0.909	21.72	87.26
	Max	0.999	0.986	35.16	208.31
	Mean	0.998	0.960	28.05	133.27
CatBoost	Min	0.999	0.918	2.92	57.58
	Max	0.999	0.991	5.53	211.34
	Mean	0.999	0.971	4.29	113.99
XGBoost	Min	0.999	0.927	10.09	57.44
	Max	0.999	0.993	14.36	181.41
	Mean	0.999	0.975	12.12	105.09

Table 2Deviation of R² over 300 random.

Δ	RF Model	GBRT Model	CatBoost Model	XGBoost Model
Min	0.002	0.012	0.009	0.007
Max	0.108	0.089	0.082	0.073
Mean	0.031	0.038	0.029	0.025

5.1. Assessment of feature importance

The results obtained from SHAP analysis, as shown in Fig. 12, provide valuable insight into the importance of each input feature for predicting the lateral strength of squat RC walls. X-axis represents a specific SHAP value, while y-axis represents the input variables sorted by importance. Dots in the graph depict the patterns in the dataset, with the colour of each dot indicating the value of the feature, where blue represents low values and red represents high values. The horizontal

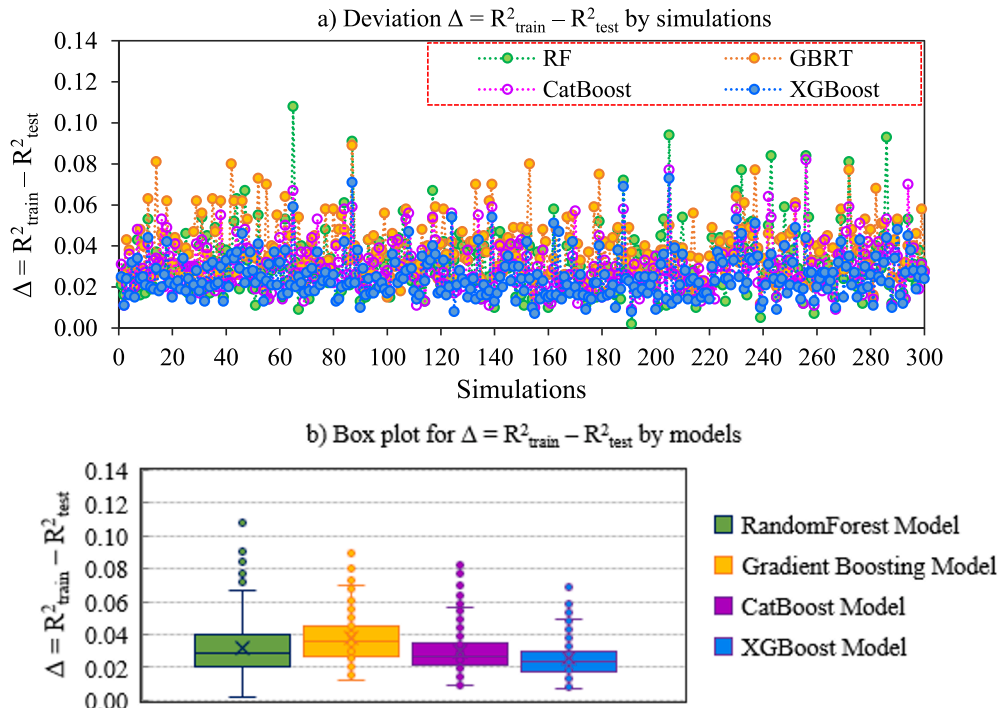
position of the dot reflects the impact of the SHAP value on the prediction.

Based on the obtained results, it can be inferred that the length of the flange and the length of the wall are the most important feature affecting the lateral strength of squat RC walls. This conclusion aligns with previous research studies that have highlighted the role of flange length in determining the structural performance of RC walls. For example, Chong et al. (2016) found that the length of the flange is an important parameter of the shear capacity of RC walls. Similarly, Kolozvari et al. (2019) demonstrated that the flange length substantially impacts the lateral strength of squat RC walls. In addition, the axial applied load is also important to the shear strength of squat RC shear walls but it was ignored in the predictive equations by ACI 318-19 (2022) and Wood (1990).

Interestingly, the influence of the longitudinal reinforcement ρ_l is more significant than that of the horizontal and vertical reinforcement (ρ_h and ρ_v) when predicting the shear strength. It's worth noting that horizontal reinforcements primarily act as shear ties, enhancing cohesion and preventing buckling of vertical bars. However, given the composition of our dataset, other features, like the vertical reinforcement and the intrinsic shear capacity of concrete, might have overshadowed the horizontal reinforcement's contribution. This observation does not undermine the essential structural role of horizontal reinforcement but underscores its relative influence within the context of this specific dataset.

5.2. Data decompositions

One of the attractive advantages of ML-based models is that they can predict the lateral shear strength within complete inputs. This scenario is popular during the preliminary design process. Reducing the number of input features in a ML model can improve time and cost-effectiveness, mitigate overfitting, and make the model more interpretable. However, this can also negatively impact the model's accuracy if important input features are ignored. This study considers three new databases with ten, eight, and six input features based on the initial database with 13 input features and the SHAP value analysis results (Table 3). The database

**Fig. 11.** Deviation of the R² over 300 random datasets.

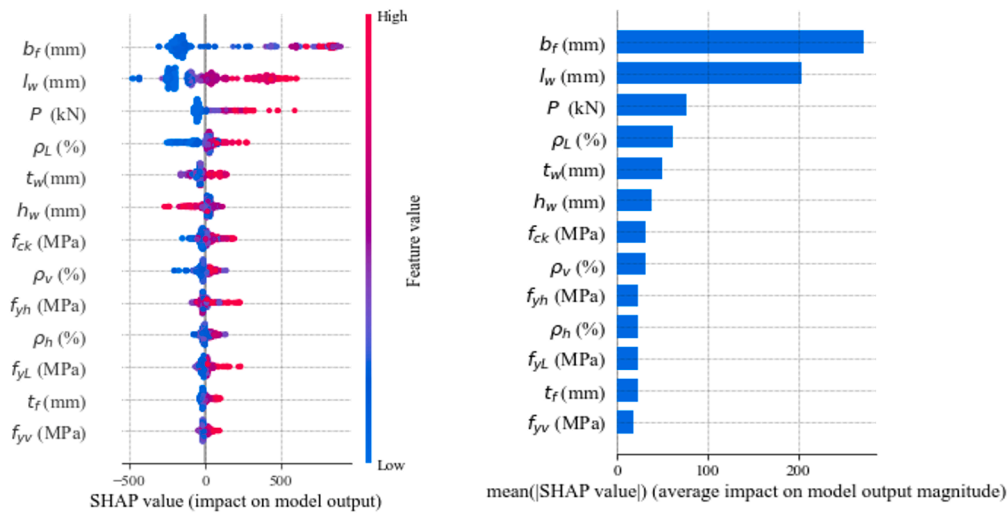


Fig. 12. SHAP values of each feature (XGBoost model).

with ten input features excluded the vertical reinforcement strength (f_{yv}), the flanged reinforcement strength (f_{yL}), horizontal reinforcement ratio (ρ_h). The database with 8 input features further excluded the strength (f_{yh}), and vertical web reinforcement ratio (ρ_v) from the ten input features database. The database with 6 input features further excluded the concrete compressive strength (f_{ck}), and flange thickness (t_f) from the 8 input features database. It is noted that excluding the concrete strength may not be a physically viable option, but this case has purely relied on the outcome in Fig. 12.

The results of Monte Carlo simulation using XGBoost model on four different datasets with varying numbers of input features were examined. The simulation involved running the model on 300 randomly divided training and testing sets, with 80–20 splits of the overall dataset containing 639 samples. A total of 1,200 simulations were conducted for these four datasets.

The results of training and testing using XGBoost model for 300 random splits of datasets with different numbers of input features are summarised in the line graph in Fig. 13, the histogram in Fig. 14, and Annex 3. The results show that, in the four investigated cases, the performance of XGBoost model for training in cases 1 and 2 is almost identical on the training, validation, and test sets. Notably, for case 2, although the number of input features is lower than that of case 1, the training performance for 300 random splits of data is slightly better. Specifically, the min/max/mean R^2 on the test set are 0.919/0.990/0.967 for case 1 and 0.936/0.990/0.969 for case 2.

For cases 3 and 4, the training results are similar, and the prediction performance is significantly worse than that of cases 1 and 2. Case 4, with the fewest input features, has the lowest model training performance. Specifically, the training performance of XGBoost model for case 4, as measured by the min/max/mean R^2 on the test set, is 0.876/0.978/0.949. Despite this result, XGBoost model can still predict the shear strength of squat walls well.

This observation highlights the importance of selecting the appropriate number of input features for a machine learning model. While more input features are often expected to improve the model's

performance, this is not always the case. The result has recommended using 10 inputs in XGBoost model to predict the shear strength of the squat RC shear wall.

5.3. Model explanation for decomposed database

The results from the SHAP analysis for the four databases with different numbers of input features indicate that the overall importance and contribution of the input features remain relatively consistent across all the four datasets (Fig. 15). However, there are some notable differences in the specific importance of certain input features. For example, the influence of " b_f " decreases as the number of input features decreases, while the influence of " l_w " increases in these cases. It is also interesting to note that the relative importance of P and t_w also seems to change across the four datasets, with P becoming more influential than t_w in the datasets with fewer input features. This suggests that while certain input features may not be important overall, they may still play a critical role in certain specific contexts.

6. Practical implications

6.1. Performances of ML models in comparison with practice codes and FEM simulation

Three semi-empirical models, Finite Element Method (FEM) and trained XGBoost model, were used to calculate the lateral strength of 639 walls. It is worth noting that FEM simulation used the non-linear pushover approach. Each simulation was stopped when a non-converged problem occurred or when the horizontal reaction at the current step of calculation was less than 80% of the maximum horizontal reaction from the previous steps. As a result, only 467 out of 639 simulations successfully calculated the lateral strength without a non-converged problem.

Table 4 reveals a clear distinction in the performance of XGBoost model across the four cases with varying numbers of input features compared to the traditional design models (ACI 318-19, ASCE/SEI 43-05, and Wood 1990) and FEM outcomes. While XGBoost model consistently outperforms the traditional design models, its performance is worse than the FEM outcomes. In the case of traditional design models, ACI 318-19 yields an R^2 of 0.522, ASCE/SEI 43-05 attains 0.544, and Wood 1990 acquires 0.426. All three design models have considerably higher RMSE, MAE, and COV values compared to XGBoost model. FEM results show remarkable performance with an R^2 of 0.998 and the lowest RMSE, MAE, and COV values among all the considered methods.

Table 3

Description of four datasets with 13, 10, 8 and 6 input features.

Name	Input features	Note
Case 1	$l_w, h_w, t_w, b_f, t_f, P, \rho_L, f_{ck}, \rho_v, f_{yv}, f_{yh}, \rho_h, f_{yL}$	Data with 13 input features
Case 2	$l_w, h_w, t_w, b_f, t_f, P, \rho_L, f_{ck}, \rho_v, f_{yh}$	Data with 10 input features
Case 3	$l_w, h_w, t_w, b_f, t_f, P, \rho_L, f_{ck}$	Data with 8 input features
Case 4	$l_w, h_w, t_w, b_f, P, \rho_L$	Data with 6 input features

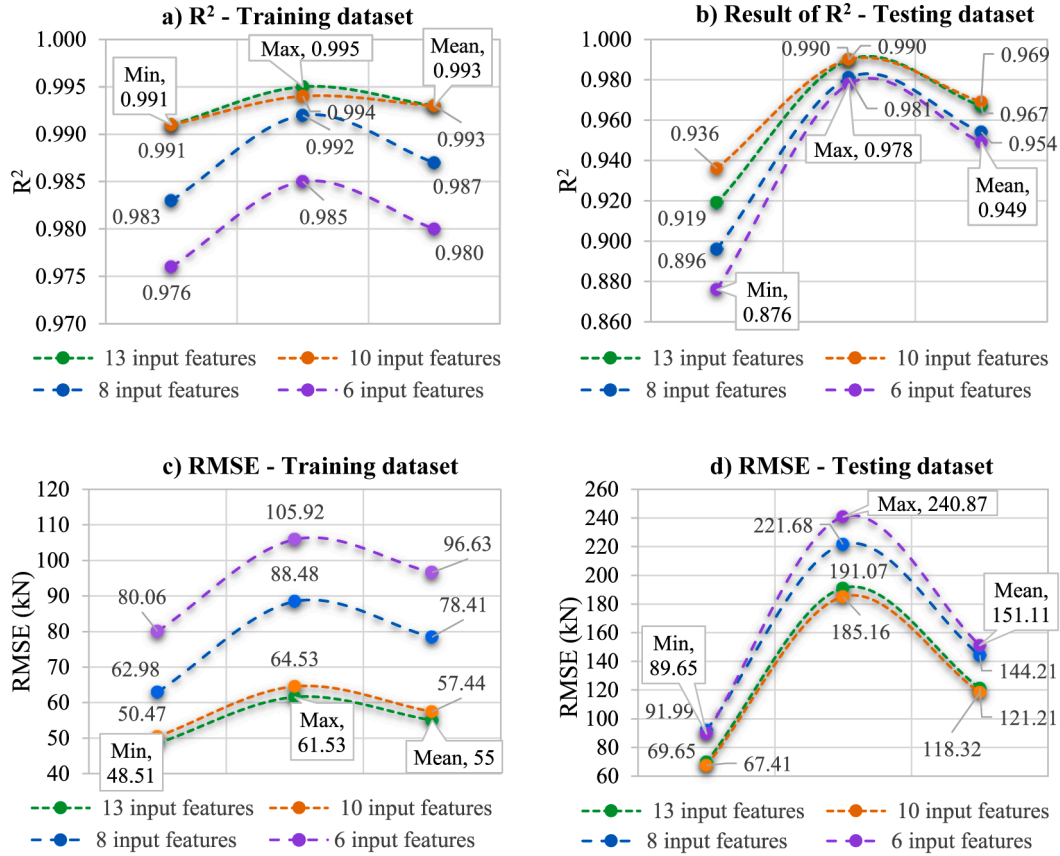


Fig. 13. R^2 and RMSE values of XGBoost model for 300 simulations.

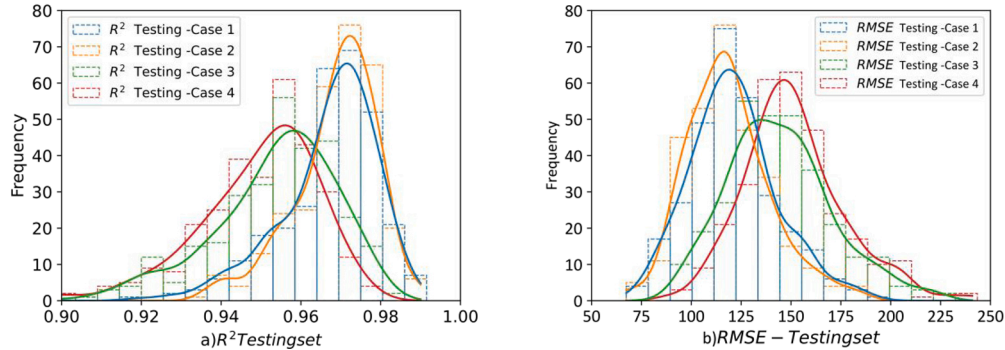


Fig. 14. Histogram R^2 and RMSE values of XGBoost model for 300 simulations.

However, FEM method is yet capable to predict all the cases in the databases.

XGBoost model maintains its superior performance with varying input features. Case 1, with 13 inputs, achieves the best results among XGBoost cases with an R^2 of 0.994, RMSE of 38.506 kN, MAE of 11.157 kN, and a COV of 18.32%. The performance remains robust in cases with fewer inputs, indicating the model's adaptability to diverse feature sets. Case 2 (10 inputs) and Case 3 (8 inputs) demonstrate only minor reductions in R^2 , while RMSE, MAE, and COV values remain relatively low compared to the traditional design standards. Even in Case 4, with only 6 inputs, XGBoost model yields an R^2 of 0.99, outperforming all traditional design models.

FEM simulations can provide high accuracy and realistic modelling of the lateral strength of squat shear walls, capturing complex non-linear

behaviour such as yielding, buckling, and cracking. However, they can also be computationally intensive and time-consuming, and the stopping criterion used in this case could result in an incomplete representation of the system, with only 467 out of 639 walls being successfully calculated without a non-converged problem, representing 73% of the database. In addition, the FEM requires a high skill and all information while the ML-based models can predict the shear strength with incomplete inputs, e.g., 10 input features, with good accuracy.

In summary, the results emphasise the potential of machine learning techniques, specifically XGBoost model, as valuable tools for predicting the lateral strength of squat shear walls in building structures. These techniques offer an appealing alternative to traditional design standards and FEM simulations, providing comparable accuracy and practical advantages in terms of computational efficiency.

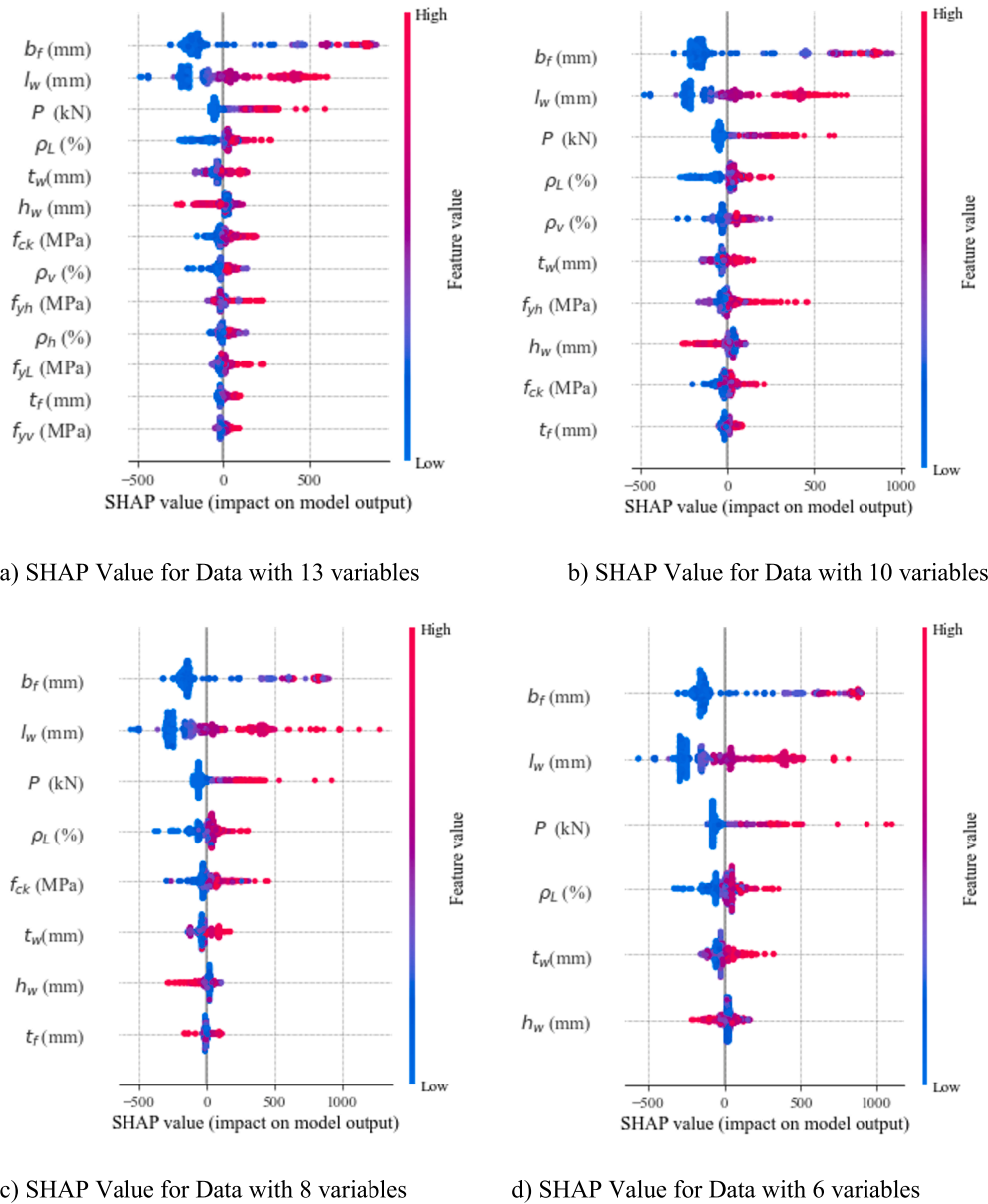


Fig. 15. SHAP value for four decompositions.

Table 4

Comparison of model performance for predicting lateral strength of squat shear walls.

Models	Result Predicted (Learn and Predict on all database)			
	R ²	RMSE (kN)	MAE (kN)	COV (%)
ACI 318–19	0.522	367.273	150.732	67.28
ASCE/SEI 43-05	0.544	358.845	136.233	60.52
Wood 1990	0.426	402.746	174.300	72.25
FEM Simulations (467 samples)	0.998	21.135	7.120	8.05
XGBoost (Data with 13 inputs – Case 1)	0.994	38.506	11.157	18.32
XGBoost (Data with 10 inputs – Case 2)	0.994	41.802	12.242	17.95
XGBoost (Data with 8 inputs – Case 3)	0.992	65.298	17.768	16.43
XGBoost (Data with 6 inputs – Case 4)	0.990	76.641	24.620	15.24

The comparison of experimental shear strength ratios for samples in the database, along with the mean and standard deviation of the prediction intervals from XGBoost model, is presented in Fig. 16. The results indicate that walls with a lower h_w/l_w ratio (≤ 1.0) exhibit a larger variation in prediction than those with a higher h_w/l_w ratio (between 1.0 and 2.0). This underlines the significance of taking the h_w/l_w ratio into account when designing walls with lower ratios.

In this study, XGBoost model demonstrates superior prediction performance relative to conventional semi-empirical models, particularly for walls with lower h_w/l_w ratios. The finding suggests that XGBoost model is particularly beneficial for estimating the shear strength of squat walls with lower h_w/l_w ratios. Consequently, incorporating XGBoost model could result in more precise predictions in the design and construction of squat walls, particularly for the case of incomplete input features, enhancing the overall reliability and safety of such structures.

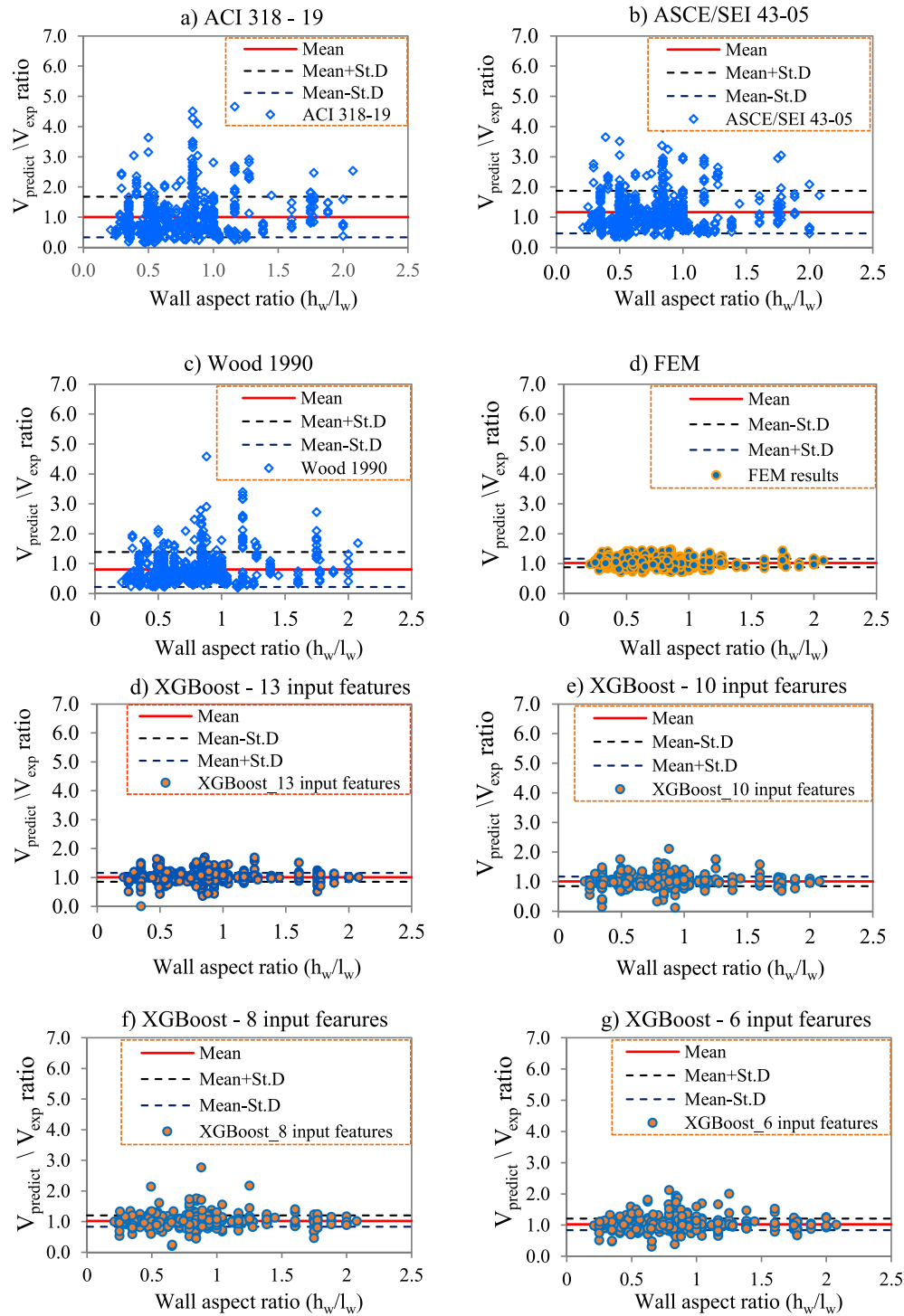


Fig. 16. Shear strength predicted by mechanics-based models: a) ACI 318 – 19; b) ASCE/SEI 43-05; c) Wood 1990; and d,e,f,g XGBoost with 13,10,8,6 input features.

6.2. Web application for predicting the lateral strength of squat shear walls

Using the Streamlit and Herokuapp frameworks, a user-friendly web application (<https://rcshearwall.herokuapp.com/>) was developed to predict the shear strength of squat shear wall using XGBoost model (Fig. 17). There are four models for predicting the shear strength of RC walls utilising input features of 13, 10, 8, and 6 that have been applied online for practical use. These application-accessible parameters correlate to the ranges of features present in the datasets used to train ML

algorithms.

Users must choose the “Prediction by XGBoost Model” button after entering values for all parameters to see the results predicted by three different models. However, it is crucial to utilise reasonable input values because employing irrational values could lead to inaccurate forecasts. Therefore, users are advised to use realistic input features.

6.3. Model limitations and scope

Our developed model, as presented in this research, has shown

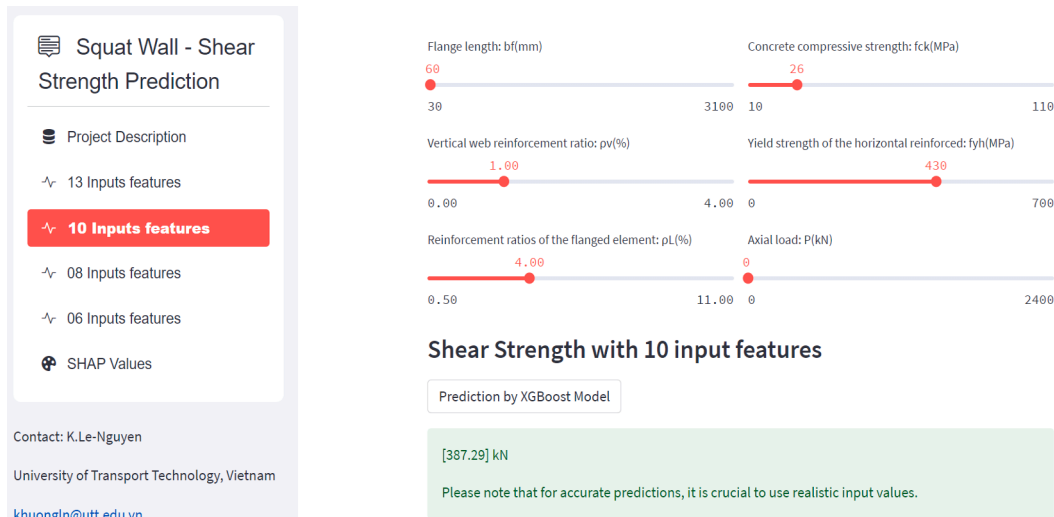


Fig. 17. Web application for predicting lateral strength using trained models.

commendable accuracy when compared to established standards. However, like all models, its predictions have boundaries governed by the scope of the data it was trained on. A difference in the representation of a given database in the reference papers compared to our dataset can cause discrepancy.

Recent studies, such as those conducted by Li et al. (2023), and Wei et al. (2022) have investigated the shear strength of specific wall configurations under seismic influences. These investigations, involving squat Ultra-High Performance Concrete (UHPC) shear walls and reinforced concrete shear walls with a low shear span ratio, provide valuable insights into the seismic behaviour of these configurations.

In our model, the axial load in the collected data is capped at $P \leq 1200$ kN. In contrast, all cases from the reference papers feature an axial load greater than 1200 kN. This limitation in our dataset means that the model may not have adequately learned the influence of higher axial loads, leading to potential discrepancies in predictions, as evidenced in the comparison of predicted outcomes with experimental data from Wei et al. (2022) presented in Fig. 18.

In future iterations of our research, we plan to address this limitation by enhancing our dataset with data from recent experimental studies, including those with higher axial loads. This expansion would enable our model to be more comprehensive and better accommodated to the evolving landscape of seismic behaviour studies, particularly with UHPC.

7. Conclusion

This study investigated the influence of input parameters on the shear strength of RC squat wall by using ML-based models and FEM. The analyses were conducted on the largest currently available dataset of 639 squat RC walls with a height-to-length ratio of less than or equal to 2.0. The findings can be summarised as follows:

- 1) The ensemble learning models, specifically XGBoost, CatBoost, GBRT, and RF, are effective in predicting the shear strength of RC squat shear walls. The use of Bayesian Optimization for hyper-parameter tuning improves the models' performance.
- 2) The results from SHAP technique indicate that the axial load has a much greater influence on the shear strength than the reinforcement ratio and compressive strength of the concrete, but it was ignored in some semi-empirical models. The influence of the longitudinal reinforcement ρ_L on the shear strength is more significant than that of the horizontal and vertical reinforcement (ρ_h and ρ_v).
- 3) Reducing the number of input features of XGBoost model from 13 to 10, 8, or 6 still yields reliable predictions with high accuracy. This suggests the robustness of this ML-based model over FEM for incomplete input parameters of RC squat walls.
- 4) XGBoost model significantly improved predictive performance compared to traditional design models such as ACI 318-19, ASCE/SEI 43-05, and Wood (1990).

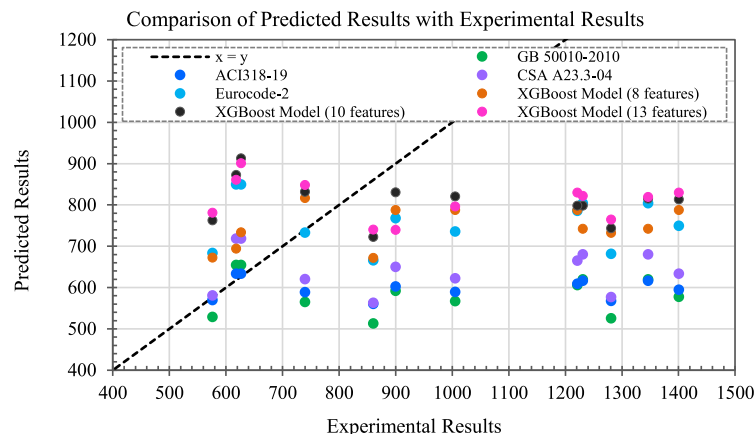


Fig. 18. Comparison of Predicted Outcomes with Experimental Data from Wei et al. (2022).

- 5) The use of XGBoost models (with various advantages such as faster computation, lower resource requirements, and efficient handling of large datasets) yields reliable prediction with comparable accuracy compared to FEM simulations with non-linear pushover analysis, which may encounter non-converged problems.
- 6) Finally, a web application incorporating XGBoost model with various input features provides valuable insights for predicting the lateral strength of squat shear walls in building structures.

CRedit authorship contribution statement

Khuong Le Nguyen: Data curation, Formal analysis, Investigation, Methodology, Software, Validation, Visualization, Writing – original draft. **Hoa Thi Trinh:** Data curation, Formal analysis, Investigation,

Methodology, Software, Validation, Visualization, Writing – original draft. **Saeed Banihashemi:** Methodology, Writing – review & editing. **Thong M. Pham:** Methodology, Formal analysis, Investigation, Writing – review & editing.

Declaration of Competing Interest

The authors declare that they have no known competing financial interests or personal relationships that could have appeared to influence the work reported in this paper.

Data availability

Data will be made available on request.

Annex

Annex 1. Learning results for models with default hyperparameters

Model	Sets	Measures			
		R ²	RMSE	MAE	MSE
DT	Training	0.999	2.77	0.43	7.7
	Validation	0.921	175.62	72.25	39280.5
	Testing	0.94	139.42	55.24	19437.4
LR	Training	0.9	201.1	165.7	40441.0
	Validation	0.85	276.9	173.2	76669.0
	Testing	0.86	218.3	151.3	47640.0
KNN	Training	0.966	130.55	63.97	17044.2
	Validation	0.93	175.31	92.72	32225.1
	Testing	0.85	218.42	102.61	47705.3
SVM	Training	0.971	108.6	60.3	11794.0
	Validation	0.91	206.8	113	42758.0
	Testing	0.95	135.8	77.2	18444.0
ANN	Training	0.986	90.3	51.6	8154.0
	Validation	0.95	150	76.2	22494.0
	Testing	0.97	100.1	57.5	10020.0
RF	Training	0.995	48.41	23.73	2343.9
	Validation	0.965	123.83	63.2	17260.6
	Testing	0.96	117.16	60.27	13725.6
AdaBoost	Training	0.948	161.47	133.32	26073.1
	Validation	0.91	199.11	162.47	41110.3
	Testing	0.86	214.34	149.71	45941.8
GBRT	Training	0.992	62.57	38.33	3915.2
	Validation	0.965	126.52	69.12	17468.6
	Testing	0.94	136.09	72.05	18520.5
CatBoost	Training	0.999	18.69	13.16	349.3
	Validation	0.976	105.84	58.66	12394.4
	Testing	0.96	115.09	59.49	13245.3
XGBoost	Training	0.999	3.46	1.85	12.0
	Validation	0.972	111.8	58.7	14580.0
	Testing	0.96	115.49	54.54	13337.2

Annex 2. The range and optimised values for 4 best-performing ML-based models

Model	Hyperparameter	Range	Optimal value
XGBoost	'n_estimators'	200–2500	1843
	'max_depth'	1–10	2
	'learning_rate'	0.01–0.99	0.3463
	'booster'	'bgtree', 'dart'	dart
	'gamma'	0.01–10	0.01
	'reg_lambda'	1–50	15
CatBoost	'iterations'	10–2000	2000
	'depth'	1–12	6
	'learning_rate'	0.01–1.0	1
	'random_strength'	1e-9–10	6.94*e-06
	'bagging_temperature'	0–1.0	1
	'loss_function'	'RMSE', 'Tweedie:variance_power = 1.5', 'Tweedie:variance_power = 1.75', 'Tweedie:variance_power = 1.25', 'Tweedie:variance_power = 1.10', 'Tweedie:variance_power = 1.9'	RMSE
	'l2_leaf_reg'	2–100	100
GBRT	'loss'	'squared_error', 'absolute_error', 'huber', 'quantile'	'squared_error'
	'learning_rate'	0.01–1.0	1
	'max_depth'	1–20	6
	'min_samples_leaf'	1–50	50
	'min_samples_split'	2–50	50
	'n_estimators'	10–300	300
	'subsample'	0.01–1.0	0.736
RF	'bootstrap'	'True', 'False'	True
	'max_depth'	10–100	52
	'max_features'	'auto', 'sqrt', 'log2'	'auto'
	'min_samples_leaf'	1–10	1
	'min_samples_split'	2–20	3
	'n_estimators'	100–2000	100

Annex 3. Statistic results of 300 simulations for 4 databases with different number of input features

Case	Result	R ² - Training	R ² - Testing	R ² - All data	RMSE Training	RMSE Testing	RMSE All data
XGBoost – 13 input features	Min	0.991	0.919	0.979	48.51	69.65	58.00
	Max	0.995	0.990	0.993	61.53	191.07	99.79
	Mean	0.993	0.967	0.988	55.00	121.21	73.6
XGBoost – 10 input features	Min	0.991	0.936	0.979	50.47	67.41	61.16
	Max	0.994	0.990	0.992	64.53	185.16	99.57
	Mean	0.993	0.969	0.988	57.44	118.32	74.12
XGBoost – 8 input features	Min	0.983	0.896	0.97	62.98	91.99	83.23
	Max	0.992	0.981	0.985	88.48	221.68	117.46
	Mean	0.987	0.954	0.98	78.41	144.21	95.88
XGBoost – 6 input features	Min	0.976	0.876	0.962	80.06	89.65	100.01
	Max	0.985	0.978	0.979	105.92	240.87	132.65
	Mean	0.98	0.949	0.974	96.63	151.11	110.29

References

- Abuodeh, O. R., Abdalla, J. A., & Hawileh, R. A. (2020). Prediction of shear strength and behavior of RC beams strengthened with externally bonded FRP sheets using machine learning techniques. *Composite Structures*, 234, Article 111698. <https://doi.org/10.1016/j.compstruct.2019.111698>
- ACI Committee 318. (2022). ACI 318.19—Building Code Requirements for Structural Concrete and Commentary.
- Antoniades, K. K., Salonikios, T. N., & Kappos, A. J. (2007). Evaluation of hysteretic response and strength of repaired R/C walls strengthened with FRPs. *Engineering Structures*, 29, 2158–2171.
- Arabzadeh, A., Soltani, M., & Ayazi, A. (2011). Experimental investigation of composite shear walls under shear loadings. *Thin-Walled Structures*, 49(7), 842–854. <https://doi.org/10.1016/j.tws.2011.02.009>
- Babaeidarabad, S., Francisco, D. C., & Antonio, N. (2014). URM walls strengthened with fabric-reinforced cementitious matrix composite subjected to diagonal compression. *Journal of Composites for Construction*, 18(2), 04013045. [https://doi.org/10.1061/\(ASCE\)CC.1943-5614.0000441](https://doi.org/10.1061/(ASCE)CC.1943-5614.0000441)
- Baek, J.-W., Park, H.-G., Shin, H.-M., & Yim, S.-J. (2017). Cyclic loading test for reinforced concrete walls (aspect ratio 2.0) with grade 550 MPa (80 ksi) shear reinforcing bars. *Structural Journal*, 114(3), 673–686. <https://doi.org/10.14359/51689437>
- Barda, F., Hanson, J. M., & Corley, W. G. (2011). *Shear strength of low-rise walls with boundary elements*. 318Reference.
- Bekő, A., Rosko, P., Wenzel, H., Pegon, P., Markovic, D., & Molina, F. J. (2015). RC shear walls: Full-scale cyclic test, insights and derived analytical model. *Engineering Structures*, 102, 120–131. <https://doi.org/10.1016/j.engstruct.2015.07.053>
- Bengio, Y., & Grandvalet, Y. (2004). No unbiased estimator of the variance of K-fold cross-validation. *Journal of Machine Learning Research*, 5(Sep), 1089–1105.
- Breiman, L. (2001). Random forests. *Machine Learning*, 45(1), 5–32. <https://doi.org/10.1023/A:1010933404324>
- Brun, M., Labbe, P., Bertrand, D., & Courtois, A. (2011). Pseudo-dynamic tests on low-rise shear walls and simplified model based on the structural frequency drift. *Engineering Structures*, 33, 796–812.
- Brun, M., Reynouard, J. M., & Jezequel, L. (2003). A simple shear wall model taking into account stiffness degradation. *Engineering Structures*, 25, 1–9.
- Brun, M., Reynouard, J. M., Jezequel, L., & Ile, N. (2004). Damaging potential of low-magnitude near-field earthquakes on low-rise shear walls. *Soil Dynamics and*

- Earthquake Engineering, 24(8), 587–603. <https://doi.org/10.1016/j.soildyn.2004.03.004>
- Cascardi, A., Micelli, F., & Aiello, M. A. (2017). An Artificial Neural Networks model for the prediction of the compressive strength of FRP-confined concrete circular columns. *Engineering Structures*, 140, 199–208. <https://doi.org/10.1016/j.engstruct.2017.02.047>
- Castaldo, P., Amendola, G., & Palazzo, B. (2017). Seismic fragility and reliability of structures isolated by friction pendulum devices: Seismic reliability-based design (SRBD). *Earthquake Engineering & Structural Dynamics*, 46(3), 425–446. <https://doi.org/10.1002/eqe.2798>
- Chen, T., & Guestrin, C. (2016). XGBoost: A scalable tree boosting system. In *Proceedings of the 22nd ACM SIGKDD international conference on knowledge discovery and data mining*, 785–794. <https://doi.org/10.1145/2939672.2939785>
- Chen, X. L., Fu, J. P., Yao, J. L., & Gan, J. F. (2018). Prediction of shear strength for squat RC walls using a hybrid ANN-PSO model. *Engineering with Computers*, 34(2), 367–383. <https://doi.org/10.1007/s00366-017-0547-5>
- Chong, X., Xie, L., Ye, X., Jiang, Q., & Wang, D. (2016). Experimental study and numerical model calibration of full-scale superimposed reinforced concrete walls with I-shaped cross sections. *Advances in Structural Engineering*, 19(12), 1902–1916. <https://doi.org/10.1177/1369433216649392>
- Collins, M., Schapire, R. E., & Singer, Y. (2000). Logistic regression, AdaBoost and Bregman distances. In *Proceedings of the thirteenth annual conference on computational learning theory*, 158–169.
- Cortes, C., & Vapnik, V. (1995). Support-vector networks. *Machine Learning*, 20(3), 273–297. <https://doi.org/10.1007/BF00994018>
- Dan, D. (2012). Experimental tests on seismically damaged composite steel concrete walls retrofitted with CFRP composites. *Engineering Structures*, 45, 338–348. <https://doi.org/10.1016/j.engstruct.2012.06.037>
- Degtyarev, V. V., & Tsavdaridis, K. D. (2022). Buckling and ultimate load prediction models for perforated steel beams using machine learning algorithms. *Journal of Building Engineering*, 51, Article 104316. <https://doi.org/10.1016/j.jobe.2022.104316>
- Deng, J., Dong, W., Socher, R., Li, L.-J., Li, K., & Fei-Fei, L. (2009). ImageNet: A large-scale hierarchical image database. *IEEE Conference on Computer Vision and Pattern Recognition*, 2009, 248–255. <https://doi.org/10.1109/CVPR.2009.5206848>
- Djerroud, M. (1992). *Contribution à l'analyse des pièces flechies en beton arme sous chargements monotone et cyclique*. INSA de Lyon.
- Dorogush, A. V., Ershov, V., & Gulin, A. (2018). CatBoost: Gradient boosting with categorical features support. *ArXiv*.
- Elshafey, A. A., Rizk, E., Marzouk, H., & Haddara, M. R. (2011). Prediction of punching shear strength of two-way slabs. *Engineering Structures*, 33(5), 1742–1753. <https://doi.org/10.1016/j.engstruct.2011.02.013>
- EN 1998-1. (2005). *Eurocode 8: Design of structures for earthquake resistance – Part 1: General rules, seismic actions and rules for buildings* (AFNOR). <http://archive.org/details/en.1998.3.2005>
- Feng, D.-C., Ren, X.-D., & Li, J. (2018). Cyclic behavior modeling of reinforced concrete shear walls based on softened damage-plasticity model. *Engineering Structures*, 166, 363–375. <https://doi.org/10.1016/j.engstruct.2018.03.085>
- Feng, D.-C., Wang, W.-J., Mangalathu, S., Hu, G., & Wu, T. (2021). Implementing ensemble learning methods to predict the shear strength of RC deep beams with/without web reinforcements. *Engineering Structures*, 235, Article 111979. <https://doi.org/10.1016/j.engstruct.2021.111979>
- Feng, D.-C., Wang, W.-J., Mangalathu, S., & Tacioglu, E. (2021). Interpretable XGBoost-SHAP machine-learning model for shear strength prediction of squat RC walls. *Journal of Structural Engineering*, 147(11), 04021173. [https://doi.org/10.1061/\(ASCE\)ST.1943-541X.0003115](https://doi.org/10.1061/(ASCE)ST.1943-541X.0003115)
- Gondia, A., Ezzeldin, M., & El-Dakhakhni, W. (2020). Mechanics-guided genetic programming expression for shear-strength prediction of squat reinforced concrete walls with boundary elements. *Journal of Structural Engineering*, 146(11), 04020223. [https://doi.org/10.1061/\(ASCE\)ST.1943-541X.0002734](https://doi.org/10.1061/(ASCE)ST.1943-541X.0002734)
- Hastie, T., Tibshirani, R., & Friedman, J. H. (2001). *The elements of statistical learning: data mining, inference, and prediction*. Springer Science & Business Media.
- Hidalgo, P. A., Jordan, R. M., & Martinez, M. P. (2002). An analytical model to predict the inelastic seismic behavior of shear-wall, reinforced concrete structures. *Engineering Structures*, 24(1), 85–98. [https://doi.org/10.1016/S0141-0296\(01\)00061-X](https://doi.org/10.1016/S0141-0296(01)00061-X)
- Hillerborg, A., Modéer, M., & Petersson, P.-E. (1976). Analysis of crack formation and crack growth in concrete by means of fracture mechanics and finite elements. *Cement and Concrete Research*, 6, 773–781.
- Hirosawa, M. (1975). *Past experimental results on reinforced concrete shear walls and analysis on them*. Building Research Institute, Ministry of Construction.
- Hochreiter, S., & Schmidhuber, J. (1997). Long short-term memory. *Neural Computation*, 9(8), 1735–1780. <https://doi.org/10.1162/neco.1997.9.8.1735>
- Hou, C., & Zhou, X.-G. (2022). Strength prediction of circular CFST columns through advanced machine learning methods. *Journal of Building Engineering*, 51, Article 104289. <https://doi.org/10.1016/j.jobe.2022.104289>
- Hsu, T. T. C., & Zhu, R. R. H. (2002). Softened membrane model for reinforced concrete elements in shear. *Structural Journal*, 99(4), 460–469. <https://doi.org/10.14359/12115>
- <https://scikit-optimize.github.io/stable/>. (2020). *Scikit-Optimize Sequential model-based optimization in Python*.
- Hwang, S.-J., & Lee, H.-J. (2002). Strength prediction for discontinuity regions by softened Strut-and-Tie model. *Journal of Structural Engineering*, 128(12), 1519–1526. [https://doi.org/10.1061/\(ASCE\)0733-9445\(2002\)128:12\(1519\)](https://doi.org/10.1061/(ASCE)0733-9445(2002)128:12(1519))
- Ile, N., & Reynouard, J. (2000). Nonlinear analysis of reinforced concrete shear wall under Earthquake loading. *Journal of Earthquake Engineering*, 4(2), 183–213.
- Junda, E., Málaga-Chuquitaype, C., & Chawgien, K. (2023). Interpretable machine learning models for the estimation of seismic drifts in CLT buildings. *Journal of Building Engineering*, 70, Article 106365. <https://doi.org/10.1016/j.jobe.2023.106365>
- Kassem, W. (2015). Shear strength of squat walls: A strut-and-tie model and closed-form design formula. *Engineering Structures*, 84, 430–438. <https://doi.org/10.1016/j.engstruct.2014.11.027>
- Keshtegar, B., Nehdi, M. L., Kolahchi, R., Trung, N.-T., & Bagheri, M. (2022). Novel hybrid machine learning model for predicting shear strength of reinforced concrete shear walls. *Engineering with Computers*, 38(5), 3915–3926. <https://doi.org/10.1007/s00366-021-01302-0>
- Keshtegar, B., Nehdi, M. L., Trung, N.-T., & Kolahchi, R. (2021). Predicting load capacity of shear walls using SVR-RSM model. *Applied Soft Computing*, 112, Article 107739. <https://doi.org/10.1016/j.asoc.2021.107739>
- Kolozvari, K., Kalbasi, K., Orakcal, K., Massone, L. M., & Wallace, J. (2019). Shear-flexure-interaction models for planar and flanged reinforced concrete walls. *Bulletin of Earthquake Engineering*, 17(12), 6391–6417. <https://doi.org/10.1007/s10518-019-00658-5>
- Kotronis, P., Mazars, J., & Davenne, L. (2003). The equivalent reinforced concrete model for simulating the behavior of walls under dynamic shear loading. *Engineering Fracture Mechanics*, 70(7–8), 1085–1097. [https://doi.org/10.1016/S0013-7944\(02\)00167-4](https://doi.org/10.1016/S0013-7944(02)00167-4)
- Le Fichoux, E. (2011). *Présentation Et Utilisation De Cast3m*. Support of CEA (<http://www-cast3m.cea.fr>). <http://www-cast3m.cea.fr/>
- Le Nguyen, K. (2015). *Contribution à la compréhension du comportement des structures renforcées par FRP sous séismes* [Ph.D thesis, INSA de Lyon]. <https://www.theses.fr/2015ISAL0020>
- Le Nguyen, K., Brun, M., Limam, A., Ferrier, E., & Michel, L. (2014). Pushover experiment and numerical analyses on CFRP-retrofit concrete shear walls with different aspect ratios. *Composite Structures*, 113, 403–418. <https://doi.org/10.1016/j.compstruct.2014.02.026>
- Le Nguyen, K., Thi Trinh, H., Nguyen, T. T., & Nguyen, H. D. (2023). Comparative study on the performance of different machine learning techniques to predict the shear strength of RC deep beams: Model selection and industry implications. *Expert Systems with Applications*, 230, Article 120649. <https://doi.org/10.1016/j.eswa.2023.120649>
- Le Nguyen, K., Truong, B. T., & Cao, M. Q. (2017). Simulation of reinforced concrete short shear walls subjected to seismic loading. In *Proceedings of the 4th Congrès International de Géotechnique - Ouvrages - Structures*, 254–262. https://doi.org/10.1007/978-981-10-6713-6_24
- Le-Nguyen, K., Minh, Q. C., Ahmad, A., & Ho, L. S. (2022). Development of deep neural network model to predict the compressive strength of FRCM confined columns. *Frontiers of Structural and Civil Engineering*, 16(10), 1213–1232. <https://doi.org/10.1007/s11709-022-0880-7>
- Li, Y.-Y., Nie, J.-G., Ding, R., & Fan, J.-S. (2023). Seismic performance of squat UHPC shear walls subjected to high-compression shear combined cyclic load. *Engineering Structures*, 276, Article 115369. <https://doi.org/10.1016/j.engstruct.2022.115369>
- Lundberg, S. M., & Lee, S.-I. (2017). A unified approach to interpreting model predictions. *Advances in Neural Information Processing Systems*, 30. <https://proceedings.neurips.cc/paper/2017/hash/8a20a8621978632d76c43dfd28b67767-Abstract.html>
- Massone, L. M., & Melo, F. (2018). General solution for shear strength estimate of RC elements based on panel response. *Engineering Structures*, 172, 239–252. <https://doi.org/10.1016/j.engstruct.2018.06.038>
- Merabet, O. (1990). *Modélisation des structures planes en béton armé sous chargement monotone et cyclique* [Ph.D thesis]. INSA de Lyon.
- Naderpour, H., Kheyroddin, A., & Amiri, G. G. (2010). Prediction of FRP-confined compressive strength of concrete using artificial neural networks. *Composite Structures*, 92(12), 2817–2829. <https://doi.org/10.1016/j.compstruct.2010.04.008>
- Nguyen, D.-D., Tran, V.-L., Ha, D.-H., Nguyen, V.-Q., & Lee, T.-H. (2021). A machine learning-based formulation for predicting shear capacity of squat flanged RC walls. *Structures*, 29, 1734–1747. <https://doi.org/10.1016/j.istruc.2020.12.054>
- Nguyen, K. L., Do, T. T., Nguyen, G. H., & Ahmad, A. (2023). Low-code application and practical implications of common machine learning models for predicting punching shear strength of concrete reinforced slabs. *Advances in Civil Engineering*, 2023, e8853122. <https://doi.org/10.1155/2023/8853122>
- Ning, C.-L., & Li, B. (2017). Probabilistic development of shear strength model for reinforced concrete squat walls. *Earthquake Engineering & Structural Dynamics*, 46(6), 877–897. <https://doi.org/10.1002/eqe.2834>
- Pedregosa, F., Varoquaux, G., Gramfort, A., Michel, V., Thirion, B., Grisel, O., ... Duchesnay, É. (2011). Scikit-learn: Machine Learning in Python. *Journal of Machine Learning Research*, 12(85), 2825–2830.
- Quinlan, J. R. (1986). Induction of decision trees. *Machine Learning*, 1(1), 81–106. <https://doi.org/10.1007/BF00116251>
- Sadegh Barkhordari, M., & Tehranizadeh, M. (2021). Response estimation of reinforced concrete shear walls using artificial neural network and simulated annealing algorithm. *Structures*, 34, 1155–1168. <https://doi.org/10.1016/j.istruc.2021.08.053>
- Sato, S., Ogata, Y., & Yoshizaki, S. (1989). Behavior of shear wall using various yield strength of rebar Part I: An experimental study. *IASMIIT. SMIRT 10 - Anaheim, CA, USA*. <http://www.lib.ncsu.edu/resolver/1840.20/29495>
- Sittipunt, C., & Wood, S. L. (1993). *Finite element analysis of reinforced concrete shear walls*. Civil Engineering Studies.
- Snoek, J., Larochelle, H., & Adams, R. P. (2012). *Practical Bayesian Optimization of Machine Learning Algorithms* (arXiv:1206.2944). arXiv. <https://doi.org/10.48550/arXiv.1206.2944>
- Sun, H., Burton, H. V., & Huang, H. (2021). Machine learning applications for building structural design and performance assessment: State-of-the-art review. *Journal of*

- Building Engineering*, 33, Article 101816. <https://doi.org/10.1016/j.job.2020.101816>
- Teng, S., & Chandra, J. (2016). Cyclic shear behavior of high-strength concrete structural walls. *ACI Structural Journal*, 113(6), 1335–1346.
- Thai, H.-T. (2022). Machine learning for structural engineering: A state-of-the-art review. *Structures*, 38, 448–491. <https://doi.org/10.1016/j.istruc.2022.02.003>
- Tran, V.-L., & Kim, S.-E. (2021). A practical ANN model for predicting the PSS of two-way reinforced concrete slabs. *Engineering with Computers*, 37(3), 2303–2327. <https://doi.org/10.1007/s00366-020-00944-w>
- Vallenas, J. M., Bertero, V., & Popov, E. P. (1979). *Hysteretic behaviour of reinforced concrete framed walls*.
- Vecchio, F. J., & Collins, M. P. (1986). The modified compression-field theory for reinforced concrete elements subjected to shear. *Journal Proceedings*, 83(2), 219–231. <https://doi.org/10.14359/10416>
- Wei, F., Chen, H., & Xie, Y. (2022). Experimental study on seismic behavior of reinforced concrete shear walls with low shear span ratio. *Journal of Building Engineering*, 45, Article 103602. <https://doi.org/10.1016/j.job.2021.103602>
- Whyte, C., & Stojadinovic, B. (2013). Hybrid simulation of the seismic response of squat reinforced concrete shear walls. *Pacific Earthquake Engineering Research Center*.
- Wood, S. L. (1990). Shear strength of low-rise reinforced concrete walls. *Structural Journal*, 87(1), 99–107. <https://doi.org/10.14359/2951>
- Yazgan, U. (2015). Empirical seismic fragility assessment with explicit modeling of spatial ground motion variability. *Engineering Structures*, 100, 479–489. <https://doi.org/10.1016/j.engstruct.2015.06.027>
- Zhang, H., Cheng, X., Li, Y., & Du, X. (2022). Prediction of failure modes, strength, and deformation capacity of RC shear walls through machine learning. *Journal of Building Engineering*, 50, Article 104145. <https://doi.org/10.1016/j.job.2022.104145>